



**NAVAL  
POSTGRADUATE  
SCHOOL**

**MONTEREY, CALIFORNIA**

**THESIS**

**UTILITY OF SATELLITE LIDAR WAVEFORM DATA IN  
SHALLOW WATER**

by

Neal Battaglia

June 2010

Thesis Advisor:  
Second Reader:

Richard C. Olsen  
David M. Trask

**Approved for public release; distribution is unlimited**

THIS PAGE INTENTIONALLY LEFT BLANK

<b>REPORT DOCUMENTATION PAGE</b>			<i>Form Approved OMB No. 0704-0188</i>
Public reporting burden for this collection of information is estimated to average 1 hour per response, including the time for reviewing instruction, searching existing data sources, gathering and maintaining the data needed, and completing and reviewing the collection of information. Send comments regarding this burden estimate or any other aspect of this collection of information, including suggestions for reducing this burden, to Washington headquarters Services, Directorate for Information Operations and Reports, 1215 Jefferson Davis Highway, Suite 1204, Arlington, VA 22202-4302, and to the Office of Management and Budget, Paperwork Reduction Project (0704-0188) Washington DC 20503.			
<b>1. AGENCY USE ONLY (Leave blank)</b>	<b>2. REPORT DATE</b> June 2010	<b>3. REPORT TYPE AND DATES COVERED</b> Master's Thesis	
<b>4. TITLE AND SUBTITLE</b> Utility of Satellite LIDAR Waveform Data in Shallow Water		<b>5. FUNDING NUMBERS</b>	
<b>6. AUTHOR</b> Neal Battaglia		<b>8. PERFORMING ORGANIZATION REPORT NUMBER</b>	
<b>7. PERFORMING ORGANIZATION NAME(S) AND ADDRESS(ES)</b> Naval Postgraduate School Monterey, CA 93943-5000		<b>10. SPONSORING/MONITORING AGENCY REPORT NUMBER</b>	
<b>9. SPONSORING /MONITORING AGENCY NAME(S) AND ADDRESS(ES)</b> N/A		<b>11. SUPPLEMENTARY NOTES</b> The views expressed in this thesis are those of the author and do not reflect the official policy or position of the Department of Defense or the U.S. Government. IRB Protocol Number _____.	
<b>12a. DISTRIBUTION / AVAILABILITY STATEMENT</b> Approved for public release; distribution is unlimited		<b>12b. DISTRIBUTION CODE</b>	
<b>13. ABSTRACT (maximum 200 words)</b>  Data from the CALIPSO satellite are analyzed for their ability to provide information about water depth. The CALIPSO LIDAR operates at 532 and 1064 nm. The 532-nm sensor measures both total power and the perpendicularly polarized intensity. Transects are studied from three geographic areas; Kure Atoll (near Midway), the Bahamas, and Sequoia National Forest. Differences in the data for two wavelengths and polarization for the 532-nm light were examined. The cross-polarized return at 532 nm was found to be strongly related to water depth. Results are compared with depth information determined by the brightness in Landsat imagery. Shallow water areas are seen to have a specific LIDAR signature based upon the ratios of backscattered light.			
<b>14. SUBJECT TERMS</b> LIDAR Waveforms, Underwater LIDAR signature, Spaceborne LIDAR			<b>15. NUMBER OF PAGES</b> 85
			<b>16. PRICE CODE</b>
<b>17. SECURITY CLASSIFICATION OF REPORT</b> Unclassified	<b>18. SECURITY CLASSIFICATION OF THIS PAGE</b> Unclassified	<b>19. SECURITY CLASSIFICATION OF ABSTRACT</b> Unclassified	<b>20. LIMITATION OF ABSTRACT</b> UU

THIS PAGE INTENTIONALLY LEFT BLANK

**Approved for public release; distribution is unlimited**

**UTILITY OF SATELLITE LIDAR WAVEFORM DATA IN SHALLOW WATER**

Neal F. Battaglia  
Civilian, United States Navy, Monterey, California  
B.S., Computer Science, Santa Clara University, 2007

Submitted in partial fulfillment of the  
requirements for the degree of

**MASTER OF SCIENCE IN APPLIED PHYSICS**

from the

**NAVAL POSTGRADUATE SCHOOL  
June 2010**

Author: Neal Battaglia

Approved by: Richard C. Olsen  
Thesis Advisor

David M. Trask  
Second Reader

Andres Larraza  
Chairman, Physics Department

THIS PAGE INTENTIONALLY LEFT BLANK

## **ABSTRACT**

Data from the CALIPSO satellite are analyzed for their ability to provide information about water depth. The CALIPSO LIDAR operates at 532- and 1064-nm. The 532-nm sensor measures both total power and the perpendicularly polarized intensity. Transects are studied from three geographic areas; Kure Atoll (near Midway), the Bahamas, and Sequoia National Forest. Differences in the data for two wavelengths and polarization for the 532-nm light were examined. The cross-polarized return at 532-nm was found to be strongly related to water depth. Results are compared with depth information determined by the brightness in Landsat imagery. Shallow water areas are seen to have a specific LIDAR signature based upon the ratios of backscattered light.

THIS PAGE INTENTIONALLY LEFT BLANK

# TABLE OF CONTENTS

<b>I.</b>	<b>INTRODUCTION.....</b>	<b>1</b>
<b>II.</b>	<b>BACKGROUND .....</b>	<b>3</b>
<b>A.</b>	<b>EARLY LIDAR.....</b>	<b>3</b>
	<b>1. Beginnings.....</b>	<b>3</b>
	<b>2. Forestry Applications .....</b>	<b>4</b>
	<b>3. Bathymetry .....</b>	<b>5</b>
	<b>4. Waveforms and Bathymetry Data.....</b>	<b>10</b>
	<b>5. Complementing Technology .....</b>	<b>15</b>
<b>B.</b>	<b>WAVEFORM LIDAR.....</b>	<b>16</b>
	<b>1. Overview .....</b>	<b>16</b>
	<b>2. Applications.....</b>	<b>18</b>
	<b>3. CALIPSO.....</b>	<b>21</b>
<b>C.</b>	<b>RESEARCH AREAS.....</b>	<b>23</b>
<b>D.</b>	<b>CALIPSO SENSOR.....</b>	<b>23</b>
	<b>1. Sensor Overview.....</b>	<b>23</b>
	<b>2. Advantages of Satellite Remote Sensing .....</b>	<b>26</b>
	<b>3. Drawbacks of CALIPSO for Water Measurements.....</b>	<b>26</b>
<b>E.</b>	<b>THEORY .....</b>	<b>29</b>
<b>III.</b>	<b>EXPERIMENTAL APPROACH .....</b>	<b>31</b>
<b>A.</b>	<b>DATA AND IMAGERY.....</b>	<b>31</b>
	<b>1. Data .....</b>	<b>31</b>
	<b>2. Interaction With Water.....</b>	<b>33</b>
<b>B.</b>	<b>PROGRAMMING .....</b>	<b>34</b>
<b>C.</b>	<b>SITE DESCRIPTIONS .....</b>	<b>34</b>
	<b>1. Kure Atoll .....</b>	<b>34</b>
	<b>2. The Bahamas .....</b>	<b>36</b>
	<b>3. Sequoias .....</b>	<b>36</b>
<b>IV.</b>	<b>SITE ANALYSES .....</b>	<b>39</b>
<b>A.</b>	<b>IDL APPROACH.....</b>	<b>39</b>
<b>B.</b>	<b>LIDAR WATER CHARACTERIZATION .....</b>	<b>39</b>
	<b>1. Water Depth .....</b>	<b>39</b>
	<b>2. Cloud Cover.....</b>	<b>39</b>
<b>C.</b>	<b>KURE ATOLL.....</b>	<b>39</b>
<b>D.</b>	<b>THE BAHAMAS.....</b>	<b>47</b>
<b>E.</b>	<b>SEQUOIAS.....</b>	<b>49</b>
<b>F.</b>	<b>COMPARISON TO SPECTRAL BRIGHTNESS.....</b>	<b>53</b>
<b>G.</b>	<b>COMPARISON TO BATHYMETRIC NATIONAL OCEAN SURVEY .....</b>	<b>54</b>
<b>V.</b>	<b>RESULTS .....</b>	<b>57</b>
<b>A.</b>	<b>CLASSIFICATION METHODOLOGY AND THRESHOLDS.....</b>	<b>57</b>
<b>B.</b>	<b>CALIPSO'S CAPABILITIES.....</b>	<b>57</b>

<b>VI.</b>	<b>SUMMARY .....</b>	<b>59</b>
<b>A.</b>	<b>THESIS RESULTS.....</b>	<b>59</b>
<b>B.</b>	<b>LIDAR SIGNATURE OF SHALLOW WATER.....</b>	<b>59</b>
<b>C.</b>	<b>UNANSWERED QUESTIONS .....</b>	<b>59</b>
<b>VII.</b>	<b>CONCLUSIONS AND FUTURE WORK.....</b>	<b>61</b>
	<b>LIST OF REFERENCES .....</b>	<b>63</b>
	<b>INITIAL DISTRIBUTION LIST .....</b>	<b>67</b>

## LIST OF FIGURES

Figure 1.	Vertical profile over land in feet (From Link, 1969, p. 196).....	4
Figure 2.	Tree as voxel structure (Reitberger, 2008, p. 218) .....	5
Figure 3.	ALH operation over water (From LaRocque, 1999) .....	7
Figure 4.	Geometry of laser into water (From LaRocque, 1999).....	7
Figure 5.	Australian tests of ALB and angle dependence (From Penny, 1986, p. 2053) .....	9
Figure 6.	Diagram of green and IR beam propagation (From Penny, 1986, p. 2053) ....	10
Figure 7.	Reflectance and fourth derivative (From Hochberg, 2000, p. 166) .....	11
Figure 8.	OWL waveform (From Cassidy, 1995, p. 123) .....	12
Figure 9.	OWL surface return and bottom return (From Cassidy, 1995, p. 123).....	13
Figure 10.	OWL waveform with surface and bottom returns close to merging (From Cassidy, 1995, p. 118).....	13
Figure 11.	Surface and bottom return from airborne LIDAR (From Guenther, 2000, p. 3) .....	15
Figure 12.	Comparison of surface bathymetry range to airborne (From Bissett, 2005) ...	16
Figure 13.	Relative intensity vs. wavelength (From Exton, 1983, p. 58).....	19
Figure 14.	Downwelling and upwelling effects in the ocean (From McLean, 1996, p. 3262) .....	19
Figure 15.	(Top) LIDAR ICESat data of the area; (Bottom) photograph of Saharan Africa (From WFF GLAS, n.d.) .....	20
Figure 16.	NASA image by Chip Trepte and Kurt Severance (From NASA CALIPSO, 2009).....	22
Figure 17.	Schematic diagram of CALIPSO system (From Winker, 2004) .....	24
Figure 18.	Satellite system and scan (From NASA CALIPSO, 2009).....	24
Figure 19.	CALIPSO 532-nm transient response (From NASA CALIPSO, 2006).....	27
Figure 20.	Red pulse transient recovery in a laboratory measurement (From NASA CALIPSO, 2006).....	28
Figure 21.	“CALIPSO’s transient response (thick blue curve) derived from surface tail/peak ratios of all land surface data, scaled to the peak value. The red, green and black curves are CALIPSO surface returns at 30-meter vertical resolution, while the surface is at different locations within the 30-meter surface bin” (From Hu et al., 2007, p. 14509). .....	29
Figure 22.	CALIPSO scene from NASA with red line representing surface and clouds seen in the air (From NASA CALIPSO, 2009) .....	32
Figure 23.	Global map with CALIPSO scan segment (From NASA CALIPSO, 2009)....	34
Figure 24.	Kure Atoll IKONOS image (From NOAA, 2009).....	35
Figure 25.	Kure Atoll Quickbird and Landsat background mosaic with depth analysis....	35
Figure 26.	Global map with Bahamas transect segment (From NASA CALIPSO, 2009) .....	36
Figure 27.	Figure of deep water near Kure Atoll .....	41
Figure 28.	Kure Atoll shallow water .....	42

Figure 29.	Ratios of Perpendicular 532-nm scatter to total backscatter for shallow water and deep water—Kure Atoll .....	42
Figure 30.	Kure Atoll averaged returned power compared vs. range bin .....	43
Figure 31.	Kure Atoll perpendicular backscatter .....	44
Figure 32.	Ratio of perpendicular backscatter to the total backscatter for Kure Atoll.....	44
Figure 33.	Kure Atoll summed ratio of perpendicular 532-nm light to total .....	45
Figure 34.	Kure Atoll summed powers of perpendicular 532-nm and total.....	46
Figure 35.	Kure Atoll Quickbird and Landsat background mosaic with depth analysis, red corresponding to shallow water and white with deep water.....	46
Figure 36.	Another Bahamas transect, with color-coded (green/red = clouds, blue = shallow water, white = deep water) regions identified.....	47
Figure 37.	Ratio of perpendicular backscatter to the total backscatter in the Bahamas....	48
Figure 38.	Bahamas “bridge” or “tail” indicating shallow water.....	49
Figure 39.	Sequoia backscatter figure over Sequoia desert.....	50
Figure 40.	Sequoia backscatter figure over Sequoia forest.....	51
Figure 41.	Sequoia backscatter ratios for both desert and forest.....	51
Figure 42.	Sequoia spectrogram.....	52
Figure 43.	Pseudo depth in black using brightness information from Landsat (over the Bahamas) compared to CALIPSO LIDAR reflectance ratios (in color). .....	53
Figure 44.	Pseudo depth from Landsat over the Bahamas compared to CALIPSO data from another transect over a more limited area (black from Landsat, and colored points from NASA CALIPSO). .....	54
Figure 45.	National Ocean Services bathymetric map with section of Figure 36 placed on top (from NOAA NGDC Web site).....	55

**LIST OF TABLES**

Table 1. Statistics for CALIPSO sensor (From NASA CALIPSO, 2009).....26

THIS PAGE INTENTIONALLY LEFT BLANK

## LIST OF ACRONYMS AND ABBREVIATIONS

ALB	Airborne LIDAR (or Laser) Bathymetry
ALPS	Airborne LIDAR Processing System
ALS	Airborne Laser Survey (or Systems)
ALS	Airborne LIDAR System
CALIOP	Cloud-Aerosol LIDAR with Orthogonal Polarization
CALIPSO	Cloud-Aerosol LIDAR and Infrared Pathfinder Satellite
DEM	Digital Elevation Model
EAARL	Experimental Advanced Airborne Research LIDAR
ENVI	ENvironment for Visualizing Images
GPS	Global Position System
HSI	Hyperspectral Imagery
ICESat	Ice, Cloud, and Land Elevation Satellite
IDL	Interactive Data Language
IMU	Inertial Momentum Unit
LIDAR	LIght Detection And Ranging
MBES	MultiBeam Echo Sounder
OWL	Ocean Water LIDAR
PMT	Photo Multiplier Tube
SHOALS	Scanning Hydrographic Operational Airborne LIDAR Survey

THIS PAGE INTENTIONALLY LEFT BLANK

## **ACKNOWLEDGMENTS**

### **Special Thanks to:**

Dr. R. C. Olsen, Naval Postgraduate School

Angela Kim, Naval Postgraduate School

Krista Lee, Naval Postgraduate School

Dave M. Trask, Naval Postgraduate School

Michelle Stephens of Ball Aerospace & Technologies Corp. provided the lab with three data sets of areas near Midway, and helped answer questions throughout the process.

Thanks to my family for their support throughout the process.

THIS PAGE INTENTIONALLY LEFT BLANK

## I. INTRODUCTION

Looking beneath the ocean's surface remotely offers navigational and tactical benefits. Today's bathymetry methods return accurate results, but require direct access to coastal areas for an extended period of time. Boats using sonar scanning and planes with LIDAR sensors perform bathymetry measurements, which assist in navigation for ships and submarines as well as help analysts, researchers, and military personnel to better understand the battlefield. However, access to perform these measurements is not available everywhere. The ability to see through the ocean's surface from space circumvents the proximity requirement and offers the advantage of being a true mode of remote sensing.

LIDAR technology has undergone rapid improvement since its invention in the 1960s and certain systems record a full waveform of data—a number of data points dense enough to actually graph a curve. Some systems also record different wavelengths and polarizations, which interact with the environment uniquely and, therefore, return different information after reflecting off surfaces and objects. This information allows researchers to see much more than a three dimensional map.

Using LIDAR data from a satellite platform has several advantages that show promise for future research. Satellites orbit the earth at a distance much further away than a plane, so the scan has a correspondingly larger scan area. The CALIPSO satellite studies aerosols and clouds, but has a LIDAR sensor, which can also look into water. CALIPSO's receiver has a polarizing element, which attenuates surface reflections. The satellite also collects data during the day and at night, so the weakest signals are received from deeper water at night when the electromagnetic noise is lower.

The CALIPSO satellite utilizes two different wavelengths (1064-nm and 532-nm) and polarization measurements for green light. The 532-nm light allows the possibility of seeing into water, and the interaction of laser light with water will also reflect light with a changed polarization. Satellites cannot, at present, perform bathymetry measurements,

however, because of a number of problems including large distances, lower available power, and data acquisition from a high velocity platform. This research explores the possibilities of using satellites for bathymetry.

Satellite LIDAR data might be used to scan large areas of the planet and identify some features, including the presence of shallow water, using the LIDAR signatures. Areas containing these features could then be further examined. Little research has been conducted in this direction. The prediction is that the 532-nm wavelength beam onboard the CALIPSO sensor will return data from both the surface and the bottom of shallow water areas. The depth of shallow water can also be determined using brightness from optical band imagery.

This thesis tests the data from the CALIPSO LIDAR sensor to see whether LIDAR signatures are capable of finding shallow water areas in the ocean. Kure Atoll and the Bahamas were used as test areas. These places both have areas of shallow water surrounded by deep water. Differences in the reflections of the 532-nm wavelength light and the 1064-nm light and, especially, the effects of polarization, determine these signatures.

The following chapters will describe background information on the evolution of LIDAR toward full waveform data, the details of analyzing CALIPSO LIDAR data, and the results of the experiment. Chapter II provides background from early LIDAR to full waveform LIDAR, and then focuses on bathymetric applications. Chapter III examines the research areas chosen and introduces the capabilities of CALIPSO, as well as describing the experimental approach and how the data was analyzed. Chapter III also includes the process to guide a user through the use of CALIPSO data in conjunction with IDL and ENVI. Chapter IV includes the details of analysis and how the CALIPSO data was characterized in each of the sites. Chapter V breaks down the results and actual capabilities of CALIPSO to produce a shallow water signature from the LIDAR data. Chapters VI and VII lay out a summary of the research and conclusions from the experiments.

## II. BACKGROUND

### A. EARLY LIDAR

#### 1. Beginnings

The technology of LIDAR has been around since the 1960s following the invention of the laser in 1958. Airborne Laser (or LIDAR) Bathymetry (ALB) came from efforts to find submarines. Hickman and Hogg (1969) also wrote an important early paper entitled, *Application of an airborne pulsed laser for near shore bathymetric measurements*, that investigated the possibility of using a blue-green laser for airborne bathymetry. The standard LIDAR equation is derived from the radar equation. The constant speed of light enables very accurate measurements of distance. These accurate distance measurements have created high quality Digital Elevation Models (DEMs) at a far lower cost than ground surveys. Smaller LIDAR sensors enable the technology to become a tool for field measurement as well as being mounted in aircraft and spacecraft. Remotely mapping an area has been useful for navigation on land and in water, as well as for military planning.

In September 1965, measurements were made by airborne LIDAR sensors over 12 test sites with different terrain types (Link, 1969). This early sensor could accurately record the ground measurements, but had difficulty with vegetation since it recorded fewer points than modern systems. "Thus, the laser profilometer system cannot accurately profile the ground surface in vegetated areas or areas with other surface features" (p. 191). The results showed promise since the, "laser profilometer system was capable of accurately measuring specific terrain features of short distances with a resolution of 0.3 ft in the vertical plane and 1.7 ft in the horizontal plane" (p. 191).

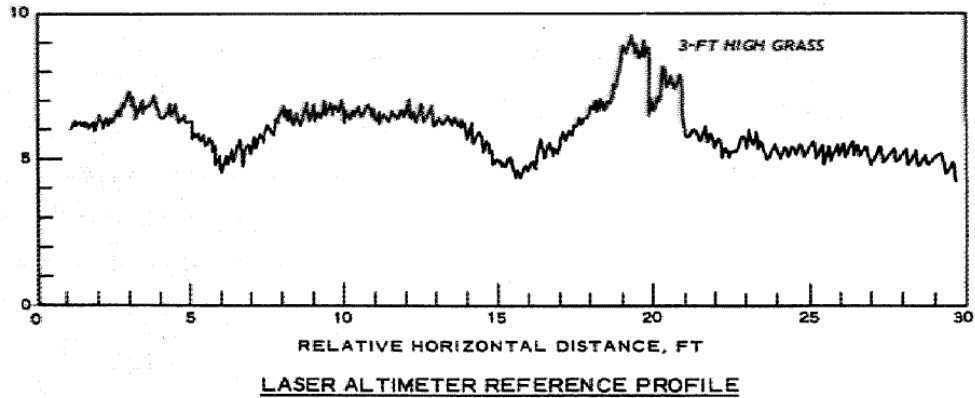


Figure 1. Vertical profile over land in feet (From Link, 1969, p. 196)

The first active LIDAR sensors carried by airborne or satellite platforms were designed at the beginning of the 1970s. The United States, Canada, Australia, and Sweden all adopted airborne LIDAR systems early in their development. These systems created one dimensional profiles (nadir view) made of sequences of single pulses. Infrared lasers became the preference for land-based LIDAR mapping whereas green laser light was added to sensors over water since it attenuates the least in coastal waters. As LIDAR systems and computers became more sophisticated, systems gained the capability to handle more data.

## 2. Forestry Applications

The forestry community has quickly adopted LIDAR for a variety of purposes. For forestry applications, researchers often assumed that the first echo belonged to the canopy top and the last pulse to the ground. Full waveform LIDAR data offered many possibilities to distinguish tree ages and species as well as characterize the structure of large forested areas. Research in forestry has helped scientists better understand the possibilities/capabilities of LIDAR. In forestry, when 3D points and their attributes are extracted from waveforms, the process yields a much larger number of points compared to just using the first and last pulses.

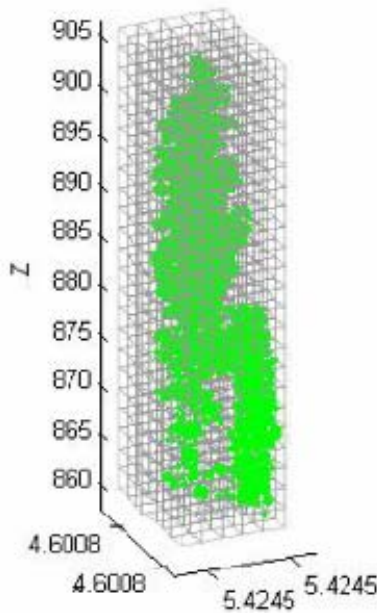


Figure 2. Tree as voxel structure (Reitberger, 2008, p. 218)

Optical sensors reveal information about forests using spectral information; however, they measure pixel values that only represent the intensity that is directly reflected from surface elements. Anything beneath the canopy surface goes unrecorded by optical sensors. The LIDAR waveform is influenced by the transmitted pulse, atmosphere, and the object being measured.

For early LIDAR returns, the first two echoes contain about 90% of the total reflected signal power; for real-time detection, more than five pulses of low intensity signals within the noise is necessary (Mallet, 2009). A single echo is sufficient for only one target within the diffraction cone (Mallet, 2009). To discriminate two objects that closely overlap, the number of samples must be high. The LIDAR data reveals different information about a scene than does classic passive imaging.

### 3. Bathymetry

Both rapid shoreline assessment for tactical military operations, and navigational charts of large areas, are performed well by airborne LIDAR. To create accurate point clouds, LIDAR uses several tools. Airborne LIDAR systems utilize Global Positioning

System (GPS) and an Inertial Momentum Unit (IMU) to record accurate spatial measurements. The IMU is used to calculate supporting vector attitudes and absolute orientation of laser sensor (Heipke et al., 2002).

Bathymetric LIDAR systems have been flown via airplanes and helicopters, but have not yet flown in space. They have been developed to carry sensors with two wavelengths. LIDAR uses both pulsed and continuous wave systems, the state-of-the-art in LIDAR focuses on pulsed systems as does this thesis. White sand in shallow water produces strong reflections, which airborne sensors can receive over a wide area. For safety purposes, the laser spreads out to an eye-safe level by the time it reaches the water's surface.

The most widely used bathymetric LIDAR in recent years has been a system designed by Optech International. The Scanning Hydrographic Operational Airborne LIDAR Survey (SHOALS) and has been widely used. The SHOALS sensor operates at 200-m altitude. Using two separate lasers has let sensors effectively measure both the surface and bottom of shallow water areas. The image of reflection curve is separated into surface, volume, and bottom. Surface detection is normally done by the infrared channel (1064-nm) while the green light (532-nm) is used to measure beneath the surface. Water clarity and turbidity are major factors in-depth determination, especially since water clarity may change quickly or be seasonally influenced.

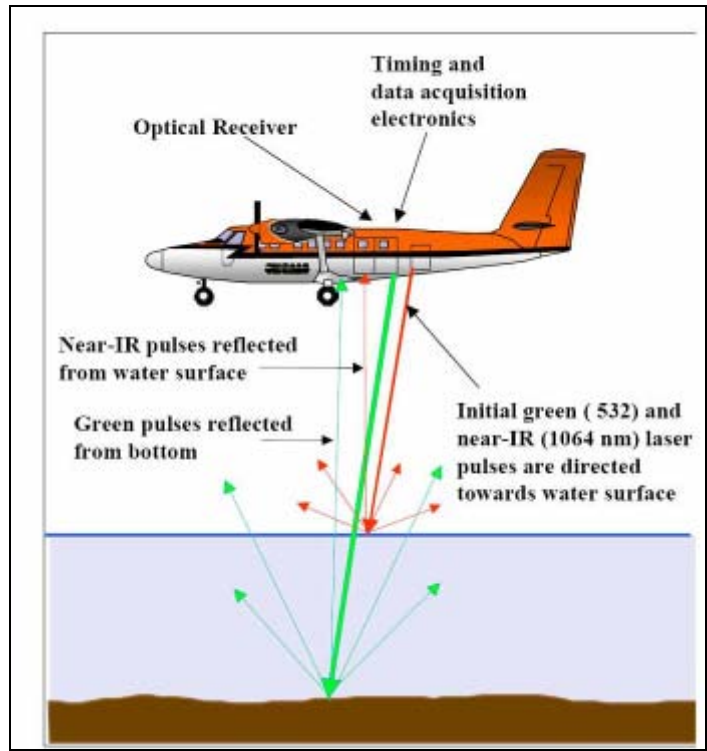


Figure 3. ALH operation over water (From LaRocque, 1999)

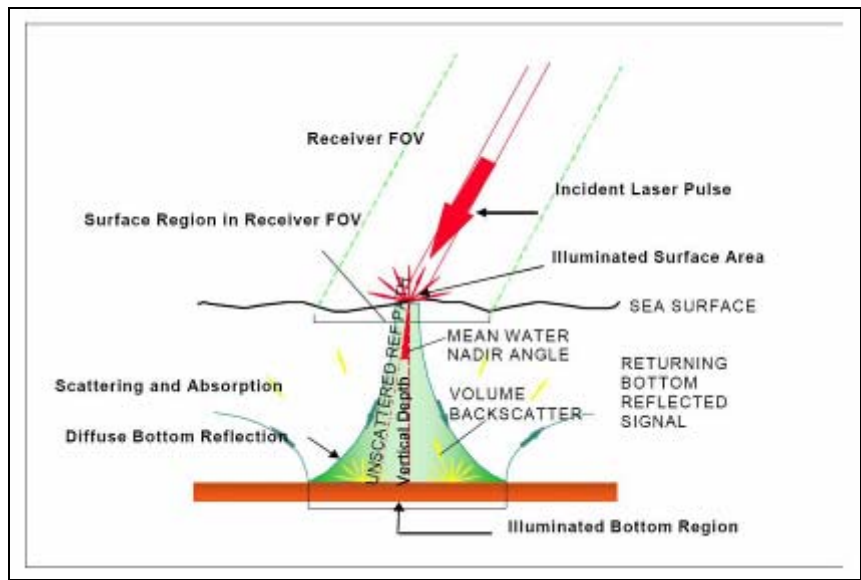


Figure 4. Geometry of laser into water (From LaRocque, 1999)

Most Airborne Laser Survey (ALS) systems only provide the coordinates of scattered objects. However, LIDAR reveals more than range information about illuminated surfaces. Green light can reach through water, while infrared light reflects off of the surface.

Bathymetric airborne LIDAR has shown promise for mapping shallow water areas quickly and with less cost than underwater surveys. The SHOALS system has proven to be a useful tool. Transmitted green lasers partially reflect from surface and bottom while the infrared lasers reflect from the surface in all but the shallowest of water. Therefore, distances can be calculated from the laser's time of travel through the air and water. Laser energy is lost because of refraction, scattering and absorption, through the water column (Irish, 1999, p. 124). Green lasers and infrared lasers are used simultaneously.

Acoustic sounding methods are the preexisting primary alternative to LIDAR bathymetry. While the techniques of interpreting airborne LIDAR data are not as developed as those for SONAR, unfamiliarity with the data from LIDAR can be overcome. Much of the energy does not return effectively to the sensor and the ratio of illumination of the target area to bottom area must be sufficiently high for detection. However, areas such as the coasts of New Zealand's Sub-Antarctic Islands have isolated pinnacles on the sea surface and extreme weather conditions. Conditions such as these make acoustic survey methods almost impossible (West, 1999). The analysis of LIDAR data using automation methods makes interpretation of the data easier to manage.

Australia has been a strong proponent of airborne bathymetry for some time now. Before the use of airborne LIDAR, acoustic methods were used to map water depths. Acoustic sounders have been in use since the 1930s and “acoustic techniques remain unchallenged in deeper waters” (Penny, 1986, p. 2046). Water turbidity strongly affects airborne bathymetry. To mitigate this problem, “knowledge of approximate water depths and the seasonal variation in water turbidity could be used to maximize the likely efficiency of a survey operation” (Penny, 1986, p. 2048). Remotely sensing aquatic areas can provide a means to plan further surveys. The maximum depth that can be measured

by sensors depends on water turbidity, laser peak power, bottom reflectivity, background light level, optical system design, and aircraft altitude. Methods for eliminating false depths have been developed.

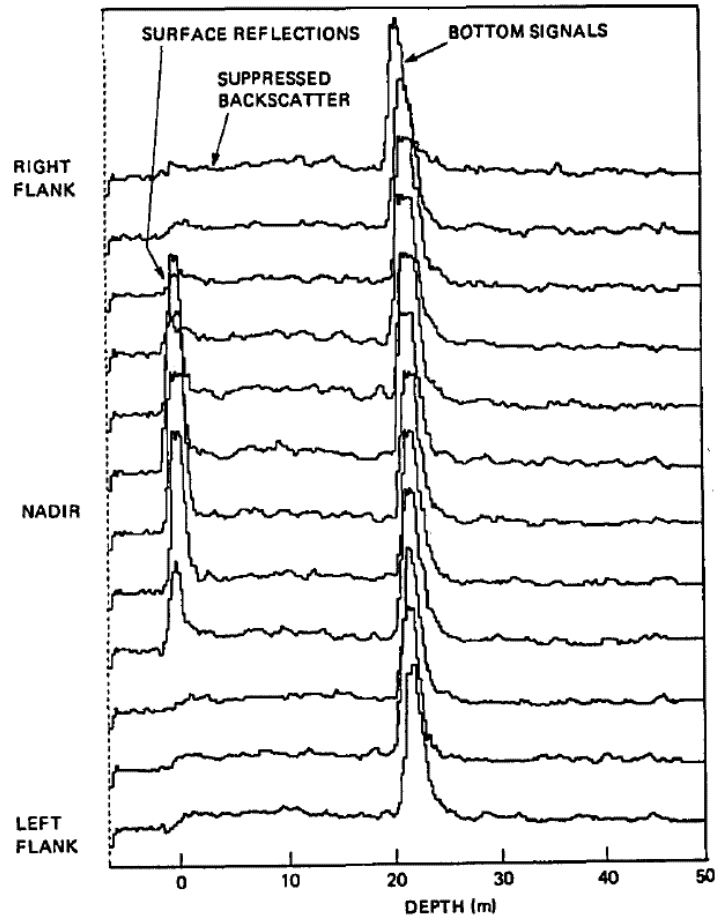


Figure 5. Australian tests of ALB and angle dependence (From Penny, 1986, p. 2053)

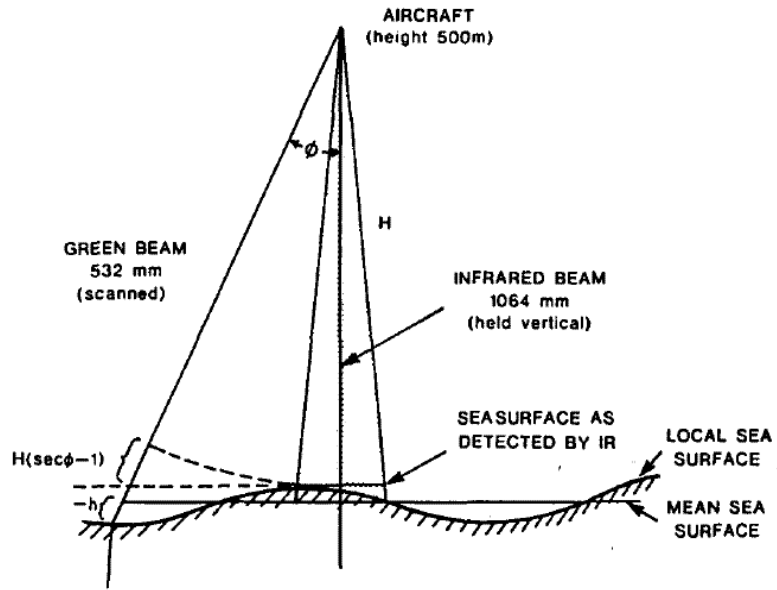


Figure 6. Diagram of green and IR beam propagation (From Penny, 1986, p. 2053)

#### 4. Waveforms and Bathymetry Data

The shape of the LIDAR waveform reveals a great deal of information beyond range measurements. For example, certain underwater features have strong signatures after taking several derivatives of the LIDAR waveform. The curve may have features that seem somewhat hidden, but are revealed by seeing the nuances of the shape by taking several derivatives. There are characteristic reflectance pattern in corals. The fourth derivative of the reflectance spectrum of coral are used to identify reflectance features since they produce sharp peaks. Analyzing LIDAR waveforms using similar techniques such may help obtain a better understanding of reef ecology. In contrast, for acoustical surveying methods, "Ground truth consisted of 144 underwater line transects" (Hochberg, 2000, p. 166). This ground truth and other sets from acoustical sensors can be very coarse.

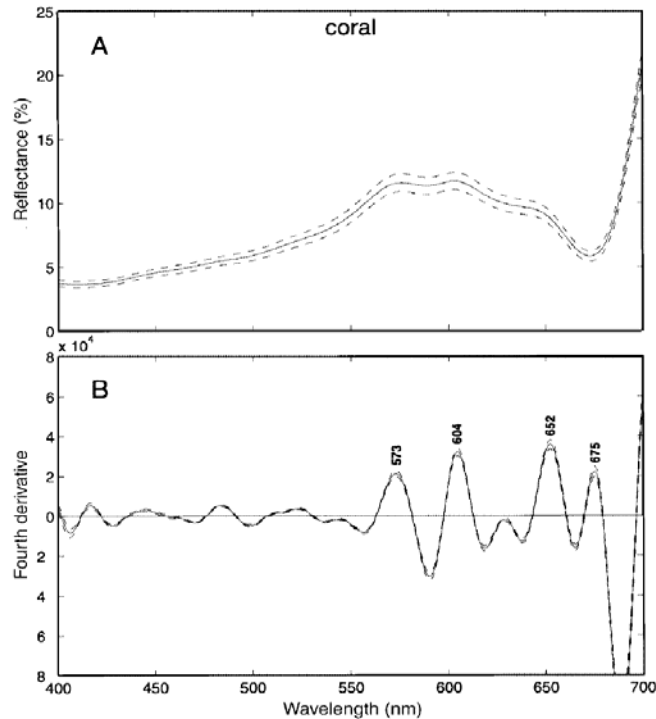


Figure 7. Reflectance and fourth derivative (From Hochberg, 2000, p. 166)

Highly sensitive LIDAR instruments, such as the Ocean Water Lidar (OWL), clearly show a signal for the bottom beneath the surface of shallow water. OWL returned a raw LIDAR waveform. Charles Cassidy performed research on this sensor, which had a primary task of testing LIDAR technology for the purpose of locating mines (Cassidy, 1995). The laser in OWL was tunable between 470-510 nm. It used a scanning mirror and the off-nadir angle was 15 degrees. OWL had an 18-20 nanosecond pulse length (full width half maximum), a beam divergence of 0.4 milliradians and a 12 meter spot size at 183 m flying altitude. Figures 8 and 9 illustrate data from the OWL sensor in shallow water near the shore. The sensor had three gain levels - low, medium, and high. The measurements are shown in two plots in Figure 8, on a linear (bottom) and logarithmic (top) scales. The left hand peak is the surface return; the right hand peak is the bottom return. The water depth at this point is approximately eight meters. Figure 9 shows a similar plot for just the low-gain channel in shallow water. Here, the water depth is about six meters. Note, that as the system moved into shallower water, the two peaks

will merge ,which is illustrated in Figure 10. Figure 10 still shows two distinct peaks, at a water depth of about four meters. The surface return has not fallen below background at the point where the bottom return begins.

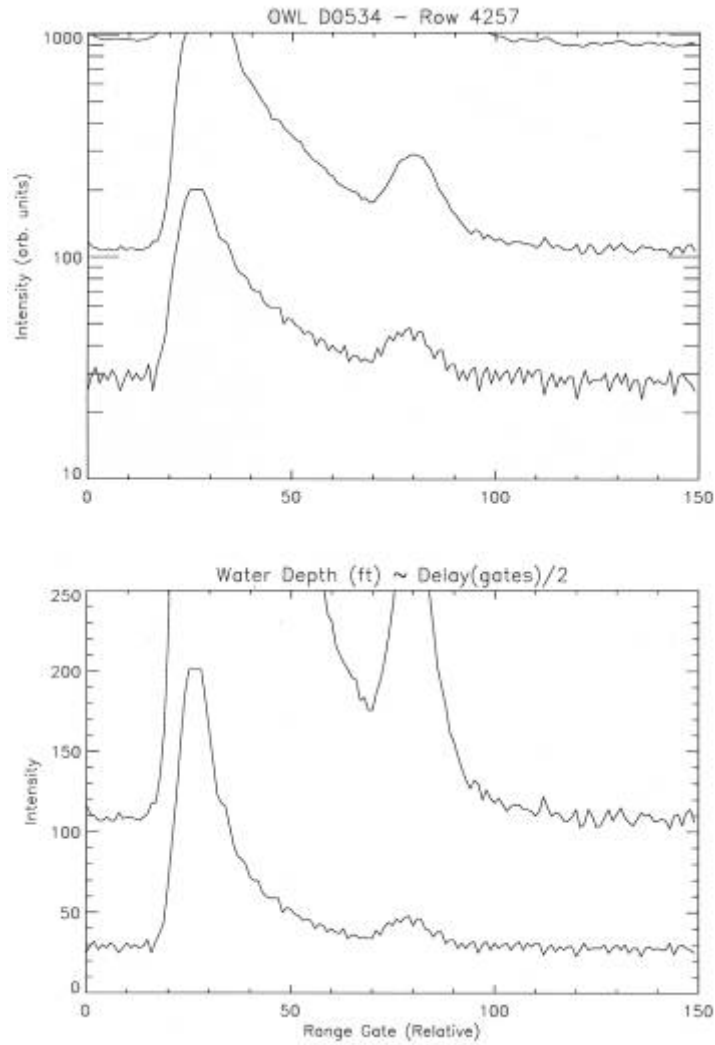


Figure 8. OWL waveform (From Cassidy, 1995, p. 123)

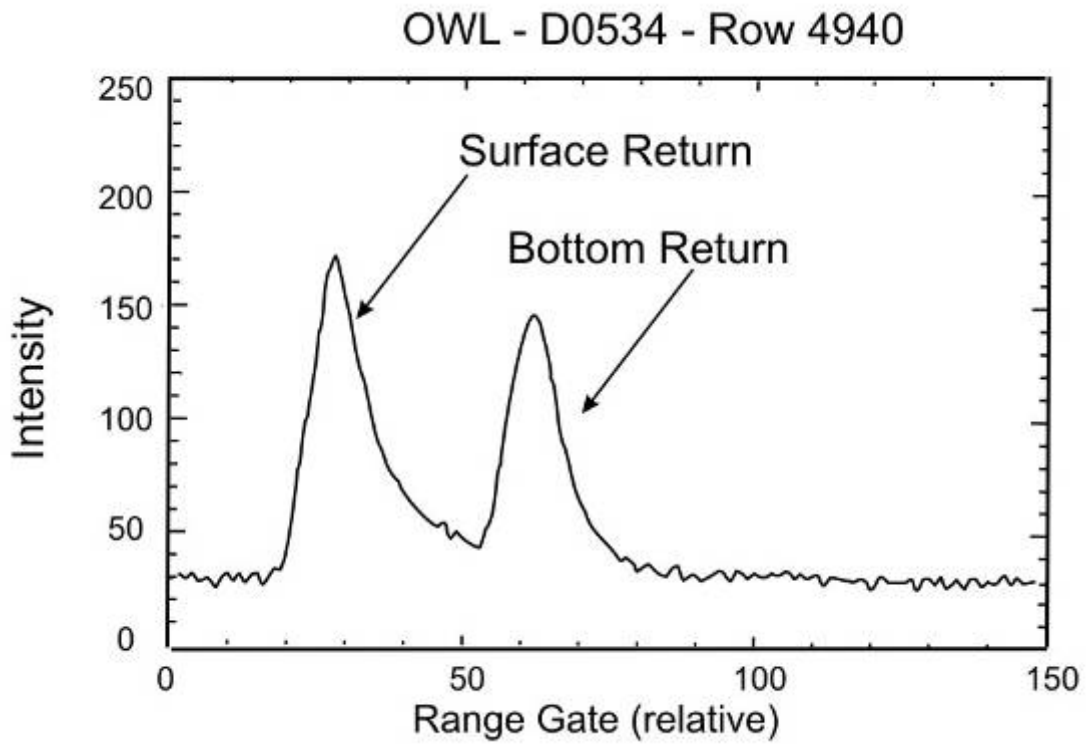


Figure 9. OWL surface return and bottom return (From Cassidy, 1995, p. 123)

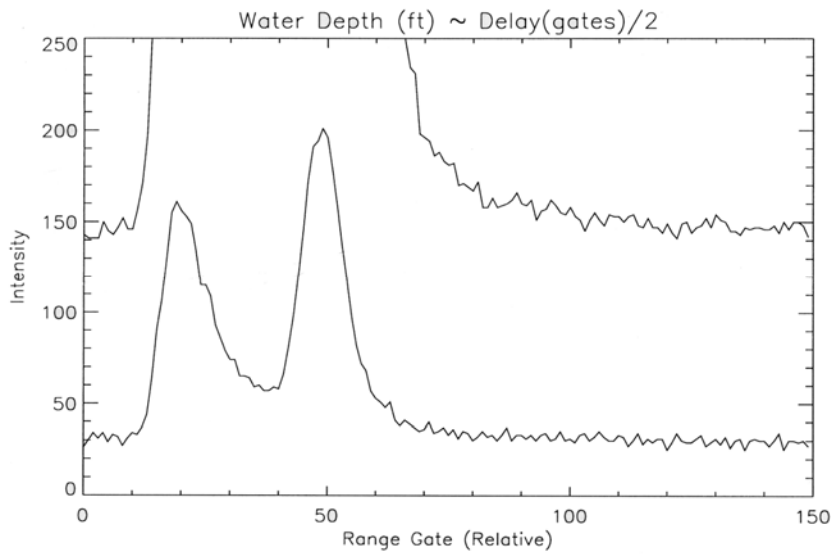


Figure 10. OWL waveform with surface and bottom returns close to merging (From Cassidy, 1995, p. 118)

A prime example of the direction that airborne bathymetry is moving can be found with the Experimental Advanced Airborne Research LIDAR (EAARL) system. This sensor builds upon the work on SHOALS. EAARL uses green light for bottom detection since it penetrates with little attenuation, but the 1064-nm wavelength is also important for various reasons. The beam spreads much more within the water, which can detract from depth accuracy, but could illuminate large bottom features. Since such a great amount of data is received by EAARL, depth is only approximately calculated in real time. Post-processing of the data then derives accurate depth measurements. EAARL does well in shallow water, but the range of LIDAR becomes limited quickly in deeper water. Ships and boats using acoustic techniques, conversely, effectively map deeper water, but have difficulty accessing shallow water areas. Airborne LIDAR can identify danger to surface vessels for sonar surveys. Airborne Laser Bathymetry (ALB) (also known as Airborne Laser Hydrography ALH) can be complemented with surface sonar bathymetry and vice versa.

EAARL uses two laser wavelengths (532-nm and 1064-nm), and the IR wavelength has proven to be very effective for terrestrial LIDAR measurements. “However, commensurate progress in bathymetry has not occurred and water remains a difficult medium through which to make remote measurements of topography” (McKean, 2009, p. 9). EAARL uses lower power, but high repetition of pulses.

EAARL can survey depths up to about 50 m (Guenther, 200, p. 5) and the ratio of absorption to scattering depends upon particles in the water. To reach beyond the surface, green light is used, but infrared (IR) light plays an important role in surface detection. Therefore an Nd:YAG Laser with a frequency doubler is used in CALIPSO and many other systems. The green light alone cannot be used for accurate surface detection since in shallow water a strong green bottom return can overpower the green surface return. Light attenuates exponentially, so the bottom return can be six or seven orders of magnitude weaker than the amplitude of the surface return. “ALH is not a substitute for side-scan sonar. Its spatial resolution is not as good as for modern high-frequency sonars, and, as noted above, some small targets may not be detected, even if illuminated.” (Guenther, 2000, p. 6) Energy backscatters from particles just below the

surface for green light as well (Guenther, 2000, p. 8). The IR can reflect off of “spray, birds, and low-lying mist,” (Guenther, 2000, p. 9) so the green return assists in determining the surface. Logarithmic amplifiers are one solution for distinguishing weak signals.

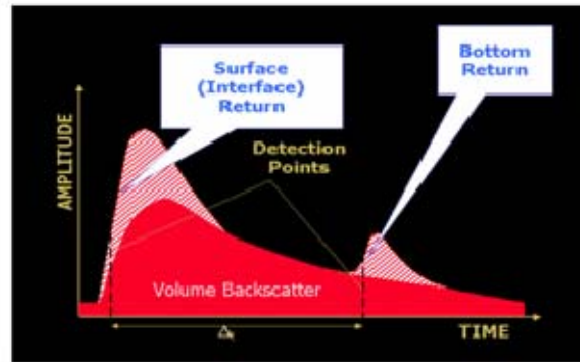


Figure 11. Surface and bottom return from airborne LIDAR  
(From Guenther, 2000, p. 3)

EAARL exemplifies how the hardware and software have been optimized for this purpose of looking at shallow water. EAARL's features include a relatively short 1.3 ns pulse, a narrow FOV (1.5-2 mrad), digitized signal temporal backscatter amplitude waveforms, and software implementation of signal-processing. EAARL also has ideal characteristics for shallow reef substrates since it has high spatial accuracy (20-cm surface footprint at 300-m altitude) and 1-ns digitizing interval resolution.

Traditional hydroacoustic ship instruments cannot operate in water more shallow than five meters, and field surveys require substantial time and funding. To assess and interpret the myriad data from EAARL, semi-automated statistical filtering methods for false bottom returns and outliers have been useful. Birds, multiple atmospheric effects, or multiple reflections from bright targets can produce surprising results (EAARL, 2009).

## 5. Complementing Technology

The use of other technologies in conjunction with LIDAR can provide a more complete set of measurements. Since LIDAR depends on water clarity and bottom reflectance characteristics, Hyperspectral Imaging (HSI) is another remote sensing

technology that can help reveal underwater environments. LIDAR systems fly lower than HSI to return a higher point density, and according to Bissett, "LIDAR bathymetric sounding from space is also a technological hurdle, whereas high resolution HSI is a possibility" (Bissett, 2005, p. 343). Advantages of LIDAR include that it is less dependent on atmospheric and solar illumination and is more likely to return information at any point in time. It also has some of the same advantages as HSI, including constant swath over changing bathymetry, and 24/7 operations. "In addition, the bathymetric sounding is also qualified for nautical charting, whereas, the HSI has yet to achieve the same level of success" (Bissett, 2005, p. 343).

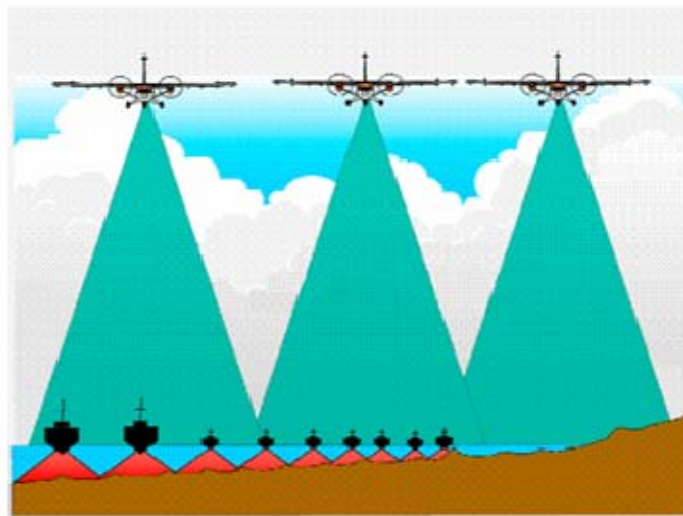


Figure 12. Comparison of surface bathymetry range to airborne (From Bissett, 2005)

## **B. WAVEFORM LIDAR**

### **1. Overview**

LIDAR creates accurate 3-Dimensional models, but LIDAR data can reveal much more than range measurements. Within the diffraction cone there are further physical properties, since light of different wavelengths interacts distinctively with the environment. The CALIPSO sensor has two wavelengths of laser—532-nm and 1064-nm. The polarization of the 532-nm light is also recorded.

Most LIDAR data undergoes processing to reduce the amount of information to a more manageable level; however, the raw data holds interesting features. Saving the complete waveform allows it to be processed and further analyzed. Computers can handle more points now, and isolating a section of a full waveform transect allows for easier processing. LIDAR is improving with hardware and micro circuitry. On land, LIDAR forest canopy penetration has undergone rapid improvement (Espinosa, 2007) and has evolved toward full waveform analysis. The complete waveform allows more control in the interpretation.

It is relatively new to actually use the full waveform. Within the full waveform there are possibilities for improving the use of LIDAR systems. Three-dimensional points and their attributes extracted from waveforms yield a very large number of points. Since work with the raw data itself is fairly new, obtaining full waveform LIDAR data is not especially common.

The shape of the LIDAR waveform curve reveals much information about the environment that has been surveyed. Keeping the raw waveforms allows further analysis following the collection. Volume backscatter reflects off of the particles in the water, and allows detection of surfaces beneath the water. That scattering also causes spreading of the laser beam, which illuminates a greater area, but also causes less energy to be returned to the sensor. The clarity of the water acts as a major limitation for LIDAR.

ALB is attractive as a means of defining safe operating areas, but it does have limits. ALB has proven accuracy, numerous/varied capabilities, high coverage, flexible, mobile, efficiency, safety, and low cost (Guenther, 2007, p. 284). However, it requires a high degree of water clarity, and distinguishing small objects is a challenge—it can resolve at most 2-meter cube objects. Things like underwater kelp can cause false bottom returns as well. The maximum depth for ALB is about 50 meters (Guenther, 2007, p. 268). LIDAR might be a good complement to traditional bathymetric mapping methods, since shallow water becomes more and more of a problem for surface ships as they approach the shore.

## 2. Applications

The airborne LIDAR systems SHOALS and EAARL have proven effective for bathymetry of shallow water areas. Knowing the underwater environment in shallow water areas applies to the military for surface navigation and submarine mapping. However, mapping shallow water proves problematic for surface vessels and there also turn out to be difficulties in distinguishing the surface and bottom returns in very shallow water from airborne LIDAR. “Mapping shallow-water bathymetry with acoustic techniques is complicated and expensive.” (Pe’eri, 2007, p. 1217) Less than 2% of the incident light is reflected as “surface return.” Green (532-nm) laser light produces returns from both the surface and bottom, but it can be difficult to distinguish the two in shallow water. For very shallow water (< 2m), it seems as though red channel can be more effective.

Bathymetry serves many useful purposes, including the detection of surface oil slicks and the detection of chlorophyll alpha using fluorescence techniques. (Exton, 1983) Suspended solids (organic and inorganic) cause scattering and absorption. Open water and coastal waters have different optimal wavelengths for maximum penetration. Light at 470-nm has minimum attenuation in open water, and light at 570-nm causes minimal attenuation in coastal waters (Exton, 1983, p. 54). Mie scattering in the ocean comes mostly from particles that are relatively large as compared to the laser wavelength. The attenuation coefficient limits the laser wavelength that can effectively be used since this coefficient increases with wavelength. Thus, proper wavelength selection can greatly increase effectiveness. The tests of multiple wavelengths for bathymetry in Exton's research included a 532.0-nm laser from Nd:YAG, similar to the sensor onboard CALIPSO. On a satellite the wavelength cannot be changed, but the 532-nm light has proven beneficial for several applications and thus continues to be installed on LIDAR sensors (Exton, 1983).

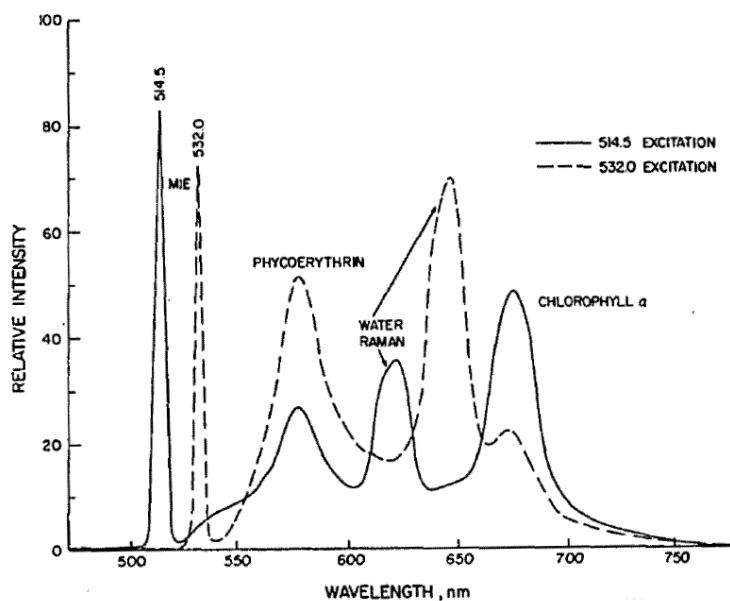


Figure 13. Relative intensity vs. wavelength (From Exton, 1983, p. 58)

Refraction at the air-sea interface can cause problems. The interface causes both downwelling irradiation effects and intensified backscatter of upwelling radiance. Spectrally dependent sensors measuring turbid waters can lead to overestimates of water reflectivity. For LIDAR, it "can lead to overestimates of the apparent diffuse attenuation and backscatter coefficients" (McLean, 1996, p. 3266).

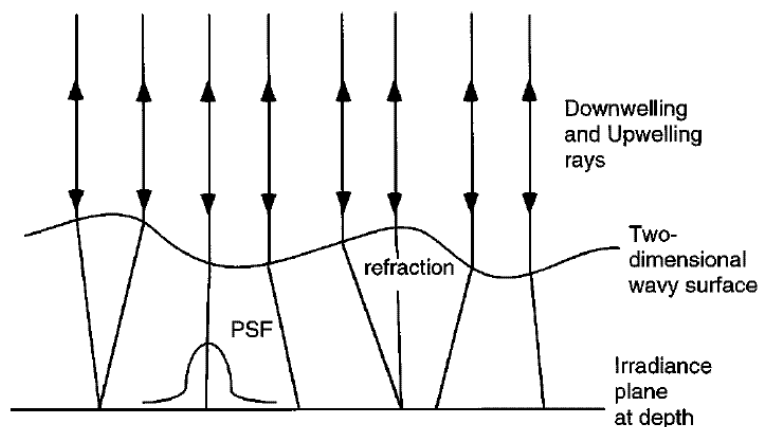


Figure 14. Downwelling and upwelling effects in the ocean (From McLean, 1996, p. 3262)

Spectral imaging can also be used to resolve depth, but only qualitatively since results do not meet hydrographic standards. Both multispectral and hyperspectral data sets can be used to estimate depths. Satellite imagery is very promising for large-scale shoreline mapping.

The NASA Ice, Cloud and land Elevation Satellite (ICESat) carried a single LIDAR sensor that measured the mass balance of the polar ice sheets. The LIDAR sensor had 1064-nm and 532-nm laser wavelengths, similar to many of the bathymetric systems. The 1064-nm light reflects from the ice surface and the 532-nm light interacts with the atmosphere. In several ways, the LIDAR onboard ICESat is similar to CALIPSO. More background on space missions using LIDAR altimetry can be found in Brian Anderson's master's thesis, 2008.

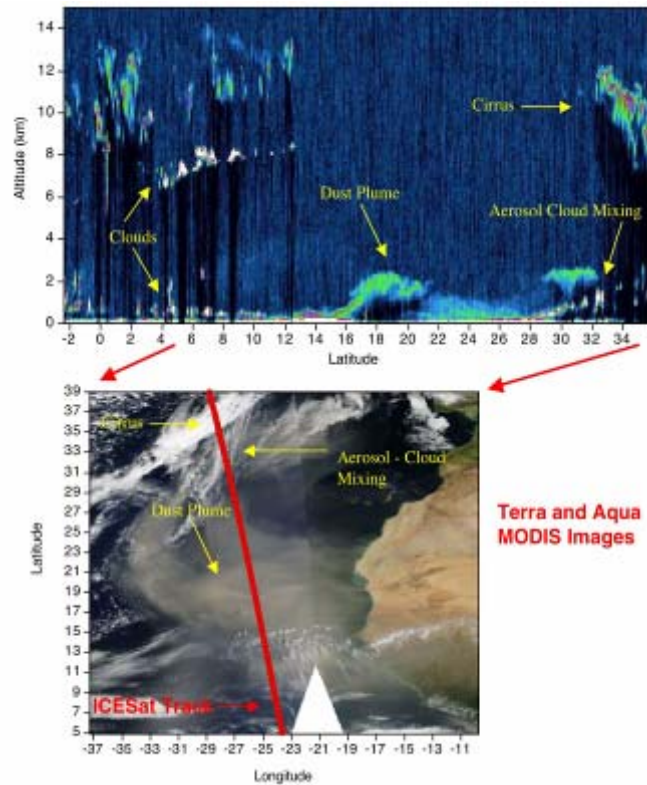


Figure 15. (Top) LIDAR ICESat data of the area; (Bottom) photograph of Saharan Africa (From WFF GLAS, n.d.)

### 3. CALIPSO

This research analyzes the utility of satellite LIDAR waveform data and polarization for shallow water areas. LIDAR can provide remote depth measurement for regions with shallow water. Measurements in these areas assist with submarine navigation. Surveying via boat and aircraft currently perform this task, but access to some areas is not always possible. This research will determine if shallow water can be identified by spaceborne LIDAR using a comparison of reflections of two laser wavelengths and polarization information.

This thesis focuses on determining the effectiveness of the spaceborne LIDAR's ability to look into shallow water. The shallow water is identified by using LIDAR data from the CALIPSO sensor. LIDAR signatures for water depth are developed using polarization information.

The two areas analyzed for this purpose were Kure Atoll, near Midway Island, and the Bahamas. Sequoia National Forest in California was used as a land based control area. Using the two sensor wavelengths and taking advantage of the polarization values for the return on the 532-nm laser, ratios of the reflection amplitudes were the main characteristic analyzed.

Ball Aerospace & Technologies Corp. provided the author with three data sets of areas near Midway. They served as a starting point. Data in raw HDF format were then downloaded through NASA's Web site. That data can be read with several programs including MATLAB and IDL. Full Waveform (FWF) LIDAR data offers a complete waveform of each backscattered pulse. The user gains more control in the interpretation process with complete waveform data and computers are now better able to handle the increased data volume.

Many LIDAR systems have a scanning mirror system that covers a broad geographic range; CALIPSO, however, does not. In an aircraft, the scanning systems are generally used because they are flown for relatively short periods of time and the scanning mirror system can be maintained or repaired. Maintaining the scanning mirror would be much more difficult on a satellite; therefore, the CALIPSO LIDAR sensor is at

a fixed angle. Since the beginning of operations in June 2006, CALIPSO has been operating with the LIDAR pointed at 0.3 degrees off-nadir (along track in the forward direction) with the exception of November 7–17, 2006 and August 21 to September 7, 2007. During these periods, CALIPSO operated with the LIDAR pointed at 3.0 degrees off nadir. Beginning November 28, 2007, the off-nadir angle will be permanently changed to 3.0 degrees.

CALIPSO thus captures on a fixed angle close to the nadir. Geographic range is sacrificed, but much higher point density is gained because all of the pulses are concentrated in this single line of data collection. The data describe a two dimensional "slice" of full waveform data, as illustrated in Figure 16.

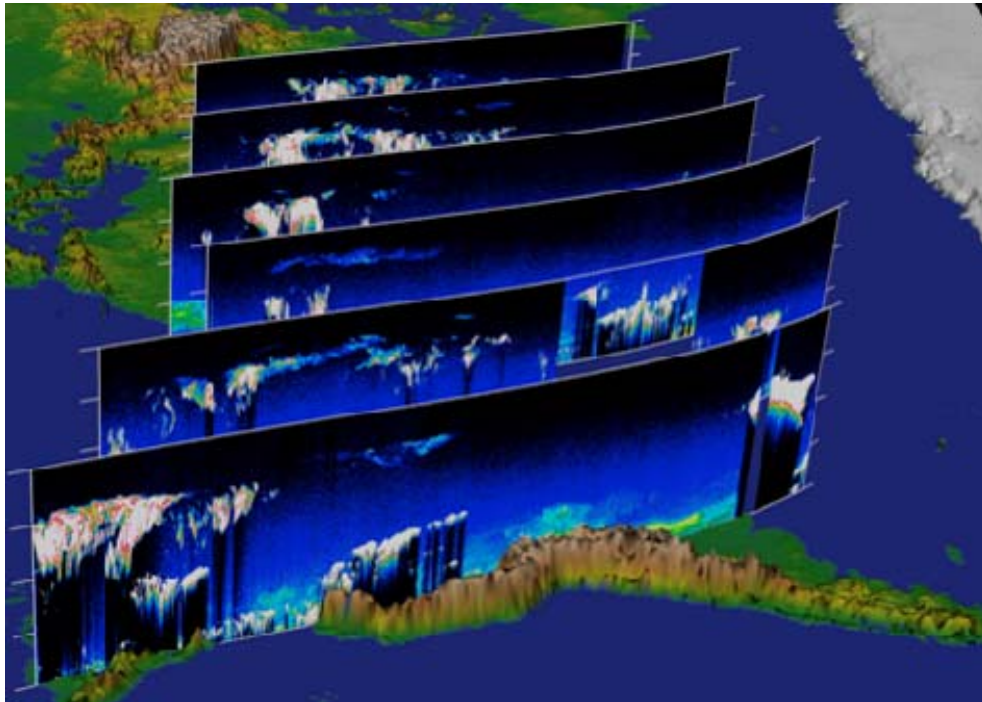


Figure 16. NASA image by Chip Trepte and Kurt Severance (From NASA CALIPSO, 2009)

## **C. RESEARCH AREAS**

The approach was to find large areas of shallow water from different areas in the world. Large and prominent shallow water areas are visible from publicly available maps and images, but many of these images do not have sufficiently small pixels to see much detail, nor do they include geographic information.

Therefore, the search was conducted within the NPS Remote Sensing Center's own data archives. Starting with islands in the Pacific Ocean: Midway, Bora Bora, and Polynesia were selected as initial sites because of prior research done within the center.

Further possibilities included: Midway, Marshall Islands, Northern Mariana Islands, American Samoa, Guam, Tuvalu, Palau, Vanuatu, Micronesia, Kiribati, Nauru, Solomon Islands, Puka Puka, Jarvis Islands, and the Johnston Atoll. Seventy-seven data sets were narrowed down to 65, based upon the extent of shallow water areas. These 65 data sets fell into 22 locations. Ball Aerospace provided CALIPSO data from Bora Bora via Matlab files derived from CALIPSO HDF files. Subsequent data came from the NASA Web site for CALIPSO data (Data tool located at [http://eosweb.larc.nasa.gov/HORDERBIN/HTML\\_Start.cgi](http://eosweb.larc.nasa.gov/HORDERBIN/HTML_Start.cgi)).

LIDAR gives the ability to look through surfaces—through canopies on land and into water, whereas photogrammetry can only see the surface. Photogrammetry does return a wealth of information about different bands of light, so LIDAR will not simply replace photogrammetry. Instead, the two technologies complement one another and give a broader spread of information about topography, bathymetry, etc. Imagery from Landsat has been used alongside the CALIPSO data in this thesis.

## **D. CALIPSO SENSOR**

### **1. Sensor Overview**

The automation of data from CALIPSO helps considerably with the analysis of clouds and aerosols. The backscatter is spectrally dependent, so the two wavelengths onboard the sensor return different information. A Boolean (true/false logic) classification approach with several variables has been taken by Mark Vaughan (2004, p. 18).

The LIDAR sensor onboard CALIPSO is the Cloud-Aerosol LIDAR with Orthogonal Polarization (CALIOP). The 532-nm and 1064-nm lasers are capable of 400 mJ per pulse; however, the power has been reduced to 110 mJ for each wavelength. This decrease in power will increase the sensor's lifetime. CALIPSO flies at an altitude of 705 km and the laser spreads to a 70 m beam diameter at the Earth's surface.

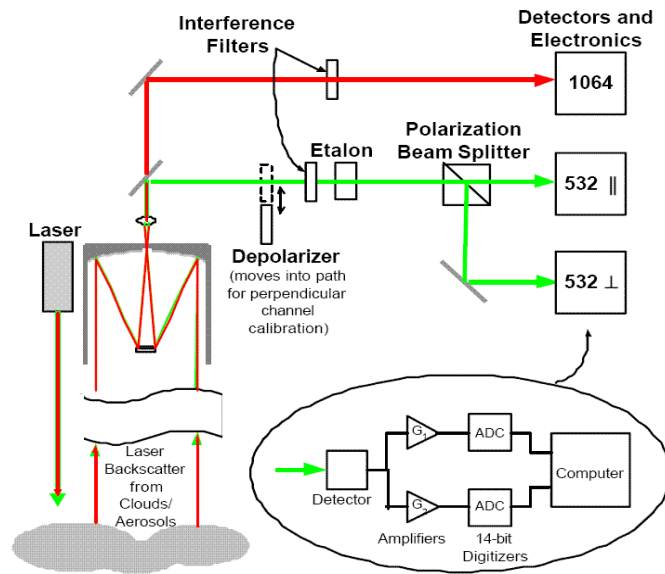


Figure 17. Schematic diagram of CALIPSO system (From Winker, 2004)

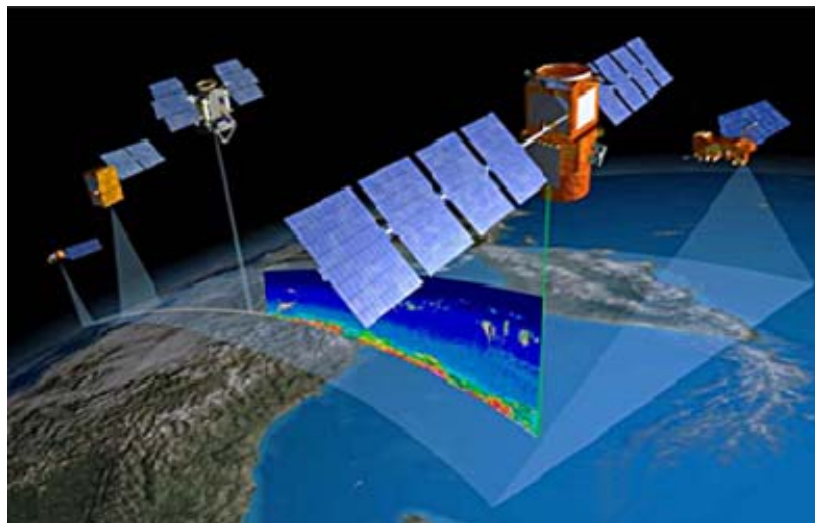


Figure 18. Satellite system and scan (From NASA CALIPSO, 2009)

CALIPSO was a joint mission with NASA and the French space agency, CNES, launched April 29, 2006. The CALIOP sensor onboard the satellite is a two-wavelength (532-nm and 1064-nm) polarization-sensitive Rayleigh-Mie LIDAR. The CALIPSO LIDAR data can be freely downloaded upon registration at NASA's Web site. On the site, users may enter in coordinates and data type specifications.

The CALIPSO sensor is equipped with a fixed angle sensor that allows full waveform data to be collected. There are two wavelengths onboard—532-nm, which has polarization, and 1064-nm. CALIPSO was designed to look at clouds and aerosols, therefore cloudy transects do not allow water measurements, because all of the LIDAR energy is reflected from the clouds and aerosols back to the sensor.

The data points are approximately 330 m apart at sea level and each data point returns a waveform of reflectance information. Since data from CALIPSO does not have the proximity of airborne LIDAR and has power limitations, it does not provide a resolution useful for bathymetry. However, the reflectance, especially of polarized green light, gives a clear indication of shallow water.

Ball Aerospace with help from Fibertek built the CALIPSO sensor. The engineering unit demonstrated a full mission lifetime (2 billion shots). Ball designed Beam Expander Optics set. Table 1 lists some statistics on CALIPSO. Not included—the pulse length, which is about 20 ns, equivalent to a length of ~6 meters. (Hu et al., 2007). This is very similar to the values for the OWL sensor, with illustrations above.

<b>Characteristics</b>	
<b>CALIOP</b>	
<b>laser:</b>	Nd: YAG, diode-pumped, Q-switched, frequency doubled
<b>wavelengths:</b>	532 nm, 1064 nm
<b>pulse energy:</b>	110 mJoule/channel
<b>repetition rate:</b>	20.25 Hz
<b>receiver telescope:</b>	1.0 m diameter
<b>polarization:</b>	532 nm
<b>footprint/FOV:</b>	100 m/ 130 $\mu$ rad
<b>vertical resolution:</b>	30-60 m
<b>horizontal resolution:</b>	333 m
<b>linear dynamic range:</b>	22 bits
<b>data rate:</b>	316 kbps

Table 1. Statistics for CALIPSO sensor (From NASA CALIPSO, 2009)

## 2. Advantages of Satellite Remote Sensing

A broad scan can identify areas of interest and places where a user might then investigate further. Spaceborne platforms deliver a much wider swath than aircraft or surface vessels. Planes also work better for LIDAR scans when flying at relatively low altitudes. Boats with sonar scans can provide much greater accuracy (image), but are not always practical because of access requirements. Satellites, therefore, have the advantage of being a true mode of remote sensing.

## 3. Drawbacks of CALIPSO for Water Measurements

CALIPSO was designed to look at clouds and aerosols. Therefore, these particles in the atmosphere interfere with measurements of water. In addition, the power available on CALIPSO does not scale up to compensate for the flying altitude. The characteristics that seem to clearly indicate shallow water using CALIPSO might also be caused by several other factors. It could be an artifact of the cross-talk between the 532-nm cross-polarized and co-polarized channels or possibly a transient response of the Photo

Multiplier Tube (PMT). "PMT afterpulsing (ionization of residual gas) is the likely cause of the non-ideal transient recovery. This effect is well documented in the literature for photon counting applications. The time scale of the effect is dependent on PMT voltage, gas species, and PMT internal geometry" (NASA CALIPSO, 2009). In Figures 19 and 20, however, the y-axis is on a logarithmic scale.

Strong backscattering targets are often associated with the non-ideal transient recoveries. The magnitude of the surface reflection for both wavelengths also depends on the wind speeds at the surface (Hu, 2008). However, the research performed for this thesis seems to validate the approach described as a technique for looking into the possibilities of satellites for LIDAR bathymetry.

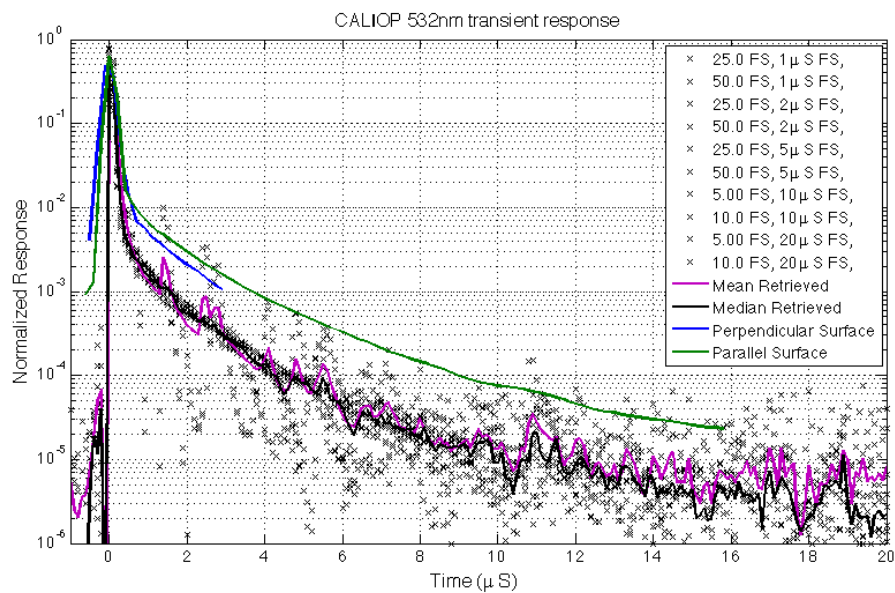


Figure 19. CALIPSO 532-nm transient response (From NASA CALIPSO, 2006)

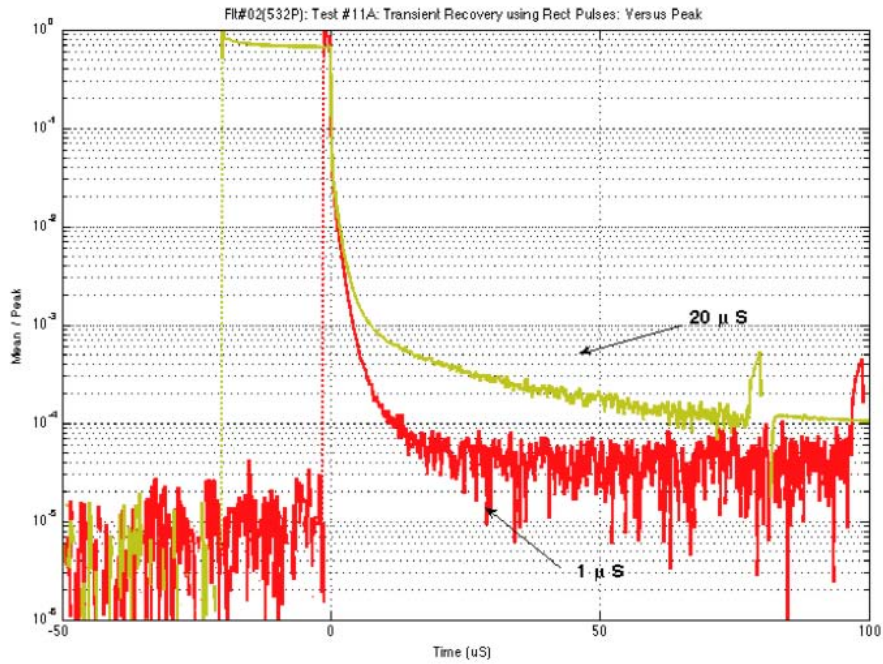


Figure 20. Red pulse transient recovery in a laboratory measurement (From NASA CALIPSO, 2006)

Hu et al., (2007) have looked at ground returns and the impact of the impulse response on altimetry. This work explores the utility of detailed analysis of the waveform return, in order to obtain finer vertical resolution for ground height measurements.

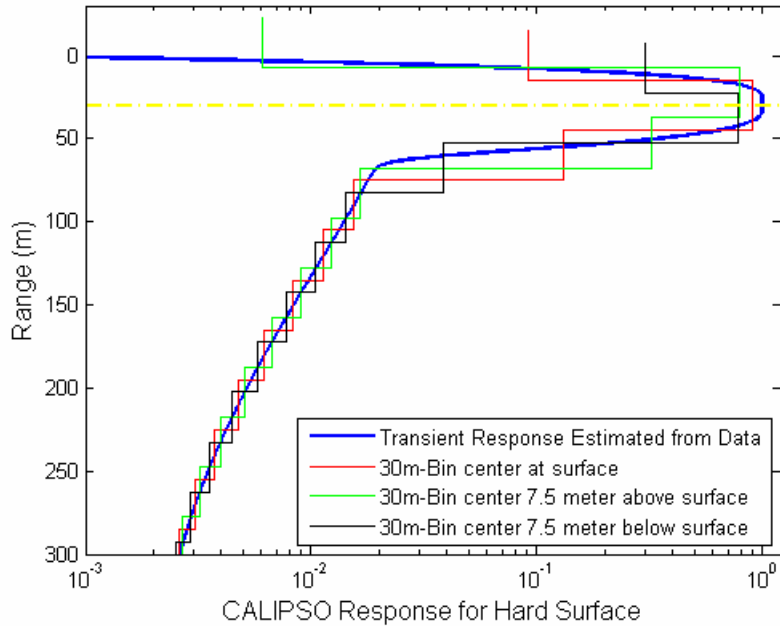


Figure 21. “CALIPSO’s transient response (thick blue curve) derived from surface tail/peak ratios of all land surface data, scaled to the peak value. The red, green and black curves are CALIPSO surface returns at 30-meter vertical resolution, while the surface is at different locations within the 30-meter surface bin” (From Hu et al., 2007, p. 14509).

## E. THEORY

The CALIPSO 1064-nm wavelength laser light will reflect off of the water's surface, whereas some of the 532-nm light will reach the bottom of the water and be reflected- thus returning information about water depth. Both co-polarized and cross-polarized green light will travel beneath the water's surface and reflect back in shallow water. The cross-polarized light gives an indication of volumetric scatter and the presence of shallow water in airborne LIDAR. A similar waveform pattern to airborne bathymetry ought to be seen in the CALIPSO data. The topic of laser interaction with water from space has not been thoroughly investigated. Since lasers traveling from satellites attenuate more than lasers from aircraft, the interaction of the CALIPSO sensor with shallow water will be the focus of this thesis.

The ENVI spectral analysis tools provide several automated processes for imagery. Mostly it is optimized for optical bands so that it can be compared to the LIDAR analysis.

### **III. EXPERIMENTAL APPROACH**

#### **A. DATA AND IMAGERY**

##### **1. Data**

NPS has acquired a rather large archive of commercial imagery. Research has been conducted near Midway Island, Hawaii, various atolls, and a number of other areas with shallow water. CALIPSO data was available for only some of these areas. Kure Atoll seemed to best serve the purpose of looking into shallow water over a mostly cloud-free area.

Overlaying the CALIPSO data over optical imagery allows for visual comparison of the LIDAR data to satellite imagery. Quickbird, IKONOS and Landsat images were used as backgrounds to overlay the CALIPSO data analysis. The optical imagery also contains brightness information, and allowed for depth analysis based upon the brightness. Mapping the analysis over an optical image allows for faster visual comparison of the LIDAR data to the visual scene.

The NASA Web site provides jpeg images of entire scans from CALIPSO transects. The transects cover the world and are broken up into four segments each. The data acquisition tool from NASA allows registered users to download these transects. A quick visual scan can identify heavy cloud cover which disrupts the laser transmission down to the ocean, as shown in Figure 22.

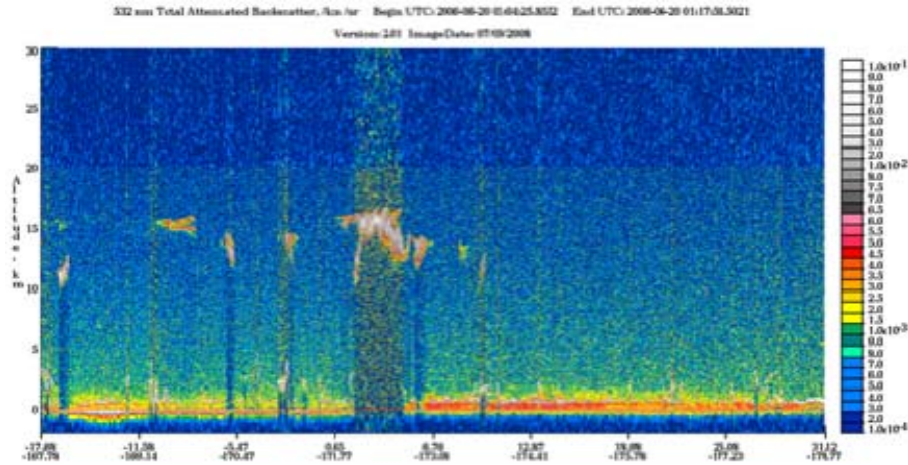


Figure 22. CALIPSO scene from NASA with red line representing surface and clouds seen in the air (From NASA CALIPSO, 2009)

Both wavelengths of laser light help with observation of water. The 532-nm beam goes through the air-water interface and propagates toward the sea bottom with lesser attenuation than the 1064-nm beam. The 532-nm data is transmitted at one polarization and then after interacting with the water, the reflection includes both the original polarization and cross polarized light. The infrared 1064-nm beam reflects off the water surface, thus returning the range from satellite or plane to sea surface. It should be noted that the night and day transects travel in opposite directions.

The CALIPSO data has been saved as Hierarchical Data Format (HDF) files. The altitude ranges between 9.0 km above sea level and 1.0 km below sea level. This range of 10 km has been divided into 583 "bins." The 583 vertical steps in waveform means each bin is about 17.15 m in vertical distance.

Several levels of data processing are available for the CALIPSO data and can be selected for download from the NASA site. This research used level 1 data (the most unprocessed). To access the CALIPSO data, registration at the Web site is the first step; then, a user may log in and select data to download.

- Select CALIPSO under Projects
- LIDAR specific data under Parameters and click "refine"
- Next a user can select the data level, in this case Level 1

- After that the user enters geographic information and time range as well as specifying Day/Night transects
- Then HDF files that match the given characteristics will be presented with file size, start/end time, and geographic information. The user has the option of downloading HDF files, metafiles, and reader files if necessary.

The cloud cover over transects can be initially analyzed using the preview images on the NASA Web site since the clouds are clearly visible in these images. The clouds block laser energy before it reaches the water. Screening the data before analysis can save time in the process.

NASA provided several sets of tools to analyze the CALIPSO data, including a tool set for IDL. These programming routines can be customized for specific tasks.

## **2. Interaction With Water**

The extent to which the laser light from the satellites will penetrate the water was unknown. From viewing the images of the CALIPSO transect segments, it seemed as though the light was reaching below the water surface. Looking into this possibility became the focus of this research.

The first geographic area to be examined was Kure Atoll near Midway Island in the Pacific Ocean. The environment there displays a high degree of homogeneity. The water depth remains fairly consistent and only a small area of land rises above the surface. When the IR (1064-nm) light hits the water, it mostly reflects off of the surface which provides a good measurement for the surface level. The green light (532-nm) will partially reflect off the surface, but more of this light will actually go beneath the surface. If the water is shallow enough, the green light will hit the bottom and then return to the sensor. The light that travels beneath the surface interacts with the water and particles within the water, thus the light that returns to the sensor changes its polarization. The polarization of the returning light therefore gives a clear signal that allows detection of shallow water.

## B. PROGRAMMING

Using modified versions of the IDL programs acting upon HDF Level 1 data, the Kure Atoll data was first checked visually, looking for differences in the waveforms for the 532-nm co-polarized and cross-polarized light and the 1064-nm light.

## C. SITE DESCRIPTIONS

### 1. Kure Atoll

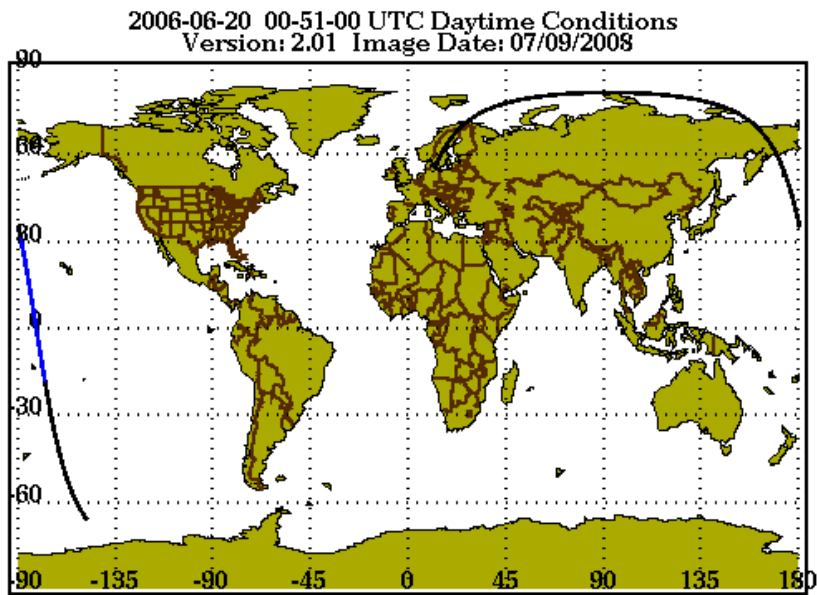


Figure 23. Global map with CALIPSO scan segment (From NASA CALIPSO, 2009)

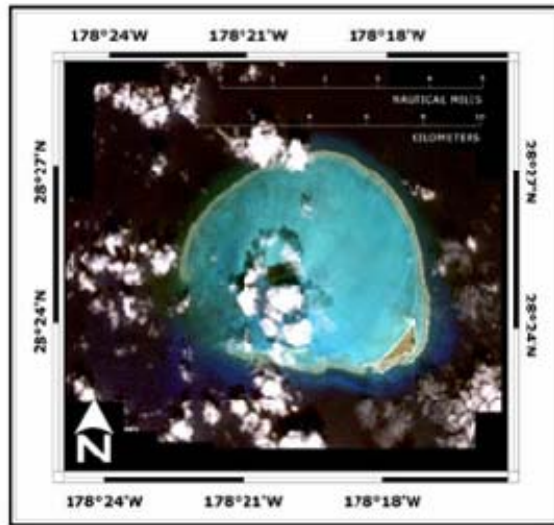


Figure 24. Kure Atoll IKONOS image (From NOAA, 2009)

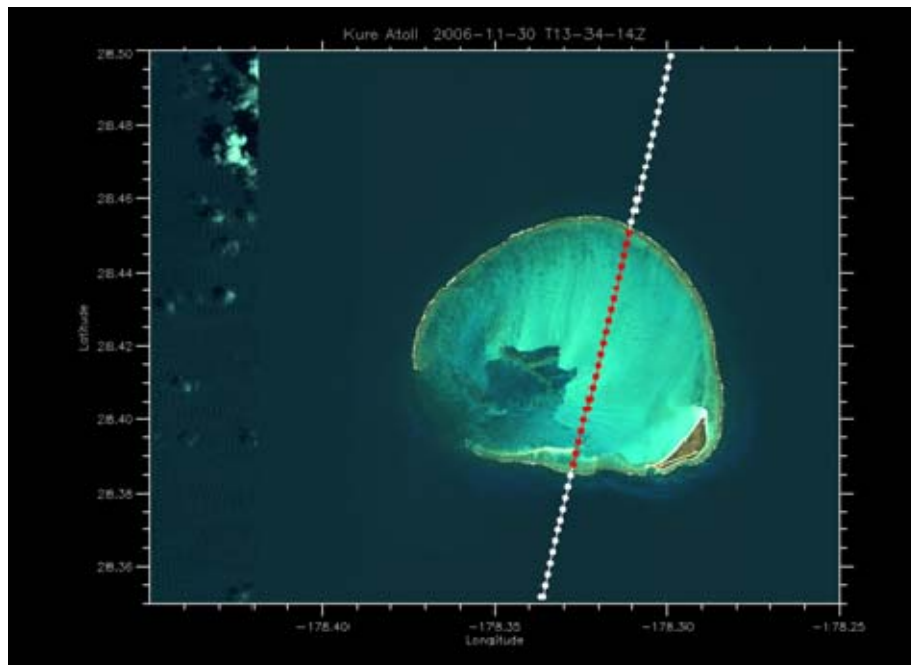


Figure 25. Kure Atoll Quickbird and Landsat background mosaic with depth analysis

Kure Atoll is located 89 km beyond Midway and is the northern-most coral atoll in the world. It consists of a 10-km wide barrier reef with a small area of land called Green Island. For this research, Kure Atoll acted as the most consistent environment

with a fairly homogeneous depth profile. Approximately 22 data points from the CALIPSO transect lie within the shallow water region of the atoll, as shown in Figure 26. Results from Kure Atoll prove to be promising for using LIDAR to identify shallow water from space.

## 2. The Bahamas

The Bahamas are located in the Atlantic Ocean north of Cuba and southeast of the United States. There are areas of shallow water, deep water, and land. The shallow water is clear and approximately 10 m deep. Compared to Kure Atoll, the Bahamas are a much larger area with greater variety in water depth and more land masses.

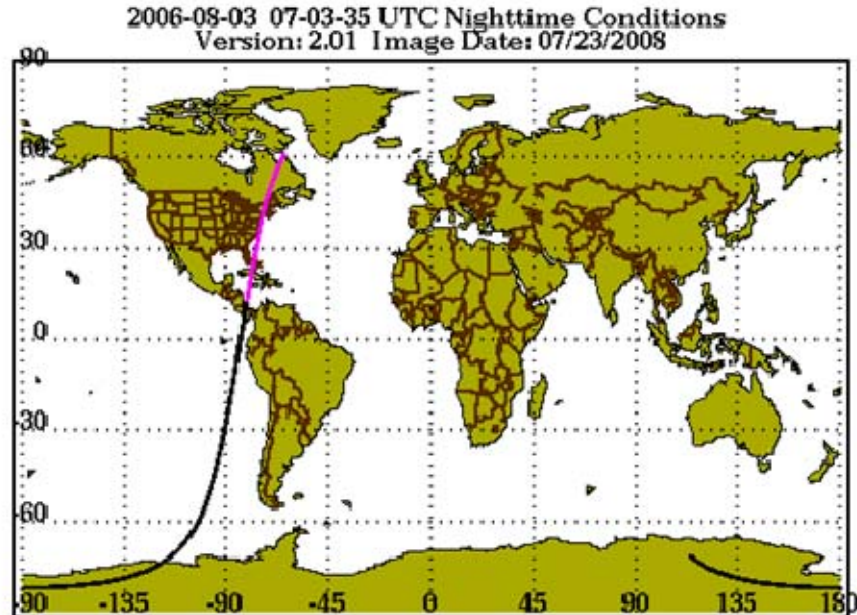


Figure 26. Global map with Bahamas transect segment  
(From NASA CALIPSO, 2009)

## 3. Sequoias

Data over land was selected to compare against the ocean and islands. Seeing LIDAR data over land confirms the unique signature for shallow water using the set of

thresholds designated to identify shallow water. The Sequoias adjacent to Sequoia National Park are located in the southern Sierra Nevada Mountains of California. There are 38 groves of Sequoia trees within the boundaries of the forest.

The trees include:

Jeffrey Pine (*Pinus jeffreyi*)

Red Fir (*Abies magnifica*)

Coast Douglas-fir (*Pseudotsuga menziesii* var. *menziesii*)

Ponderosa Pine (*Pinus ponderosa*)

White Fir (*Abies concolor*)

Lodgepole Pine (*Pinus contorta*) (Warbington, 2002).

THIS PAGE INTENTIONALLY LEFT BLANK

## **IV. SITE ANALYSES**

### **A. IDL APPROACH**

NASA provided "A set of callable routines that has been written to provide basic read access to CALIPSO science data files" (readme file). These files were modified within IDL.

The main variables that could be modified within the IDL procedures were the transect and the thresholds for the different categorization. The modified programs from NASA showed promise. Various procedures from within the original programs could be used for more complicated programming.

### **B. LIDAR WATER CHARACTERIZATION**

#### **1. Water Depth**

By comparing the ratios of 532-nm parallel and perpendicular returns to the total backscatter, shallow water could be easily distinguished. Cross polarization indicates volumetric scattering as a result of water penetration. Deeper water does not reflect the light that has entered the water and therefore has no cross-polarization component.

#### **2. Cloud Cover**

The CALIPSO sensor was designed to study clouds and aerosols, so clouds prevent clear observation of the water. The relatively unclouded transects allow the measurements of the water. Thresholds were defined to mark areas covered by cloud, allowing the measurements of the water to be immediately identified.

### **C. KURE ATOLL**

The transect progresses in time steps and the patterns of reflection can be visually scanned. Over deep water, the 532-nm light and 1064-nm light have similar levels, but different shapes, while the 532-nm cross-polarized return stays at a low level. Over

shallow water the return from the green light (532-nm) increases while the IR (1064-nm) does not change a great deal. The green light displayed a tail on falling edge, indicating that the light was traveling into the water. More noticeably, the cross-polarized green light increases a great deal over shallow water.

It seemed as if the curve would separate into two distinct returns when the green light hit the bottom of the ocean in shallow areas. That pattern has been observed in airborne bathymetry.

After discarding nearby transects and scenes with too much cloud cover, six transects for Kure Atoll were analyzed. The applicable Kure Atoll HDF transects all come from night flights. In the initial analysis, three different reflections are compared: 532-nm co-polarized, 532-nm cross-polarized, and 1064-nm.

Theoretically, it seemed as though the 532-nm light would penetrate shallow water, but the extent to which it would do so was not clear. It was predicted that the 1064-nm light would reflect off the water surface and thus provide a good comparison. In the case of deep water, both the reflected light from both wavelengths was expected to be that coming off the surface.

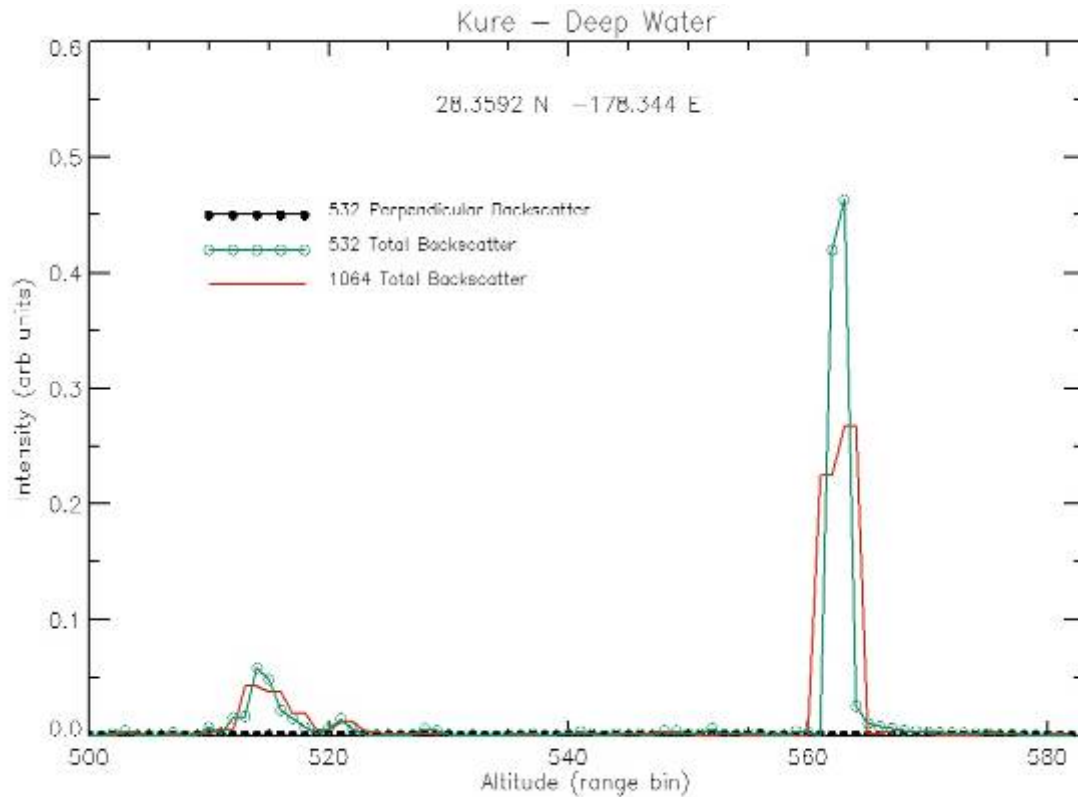


Figure 27. Figure of deep water near Kure Atoll

The modified IDL programs showed initial promise for identifying shallow water, especially with the presence of spikes in cross-polarized reflection of the green light. The file examined here is *CAL\_LID\_L1-Prov-V2-01.2008-01-04T13-33-34ZN.hdf* (Downloaded using the NASA tool on the CALIPSO Web site). Perpendicular backscatter of the 532-nm light (black in Figures 27 and 28) is the main variable of interest. The HDF transect has 56,070 elements, the deep water figure is one element (#25,598) and the shallow water is another nearby element (#25,582).

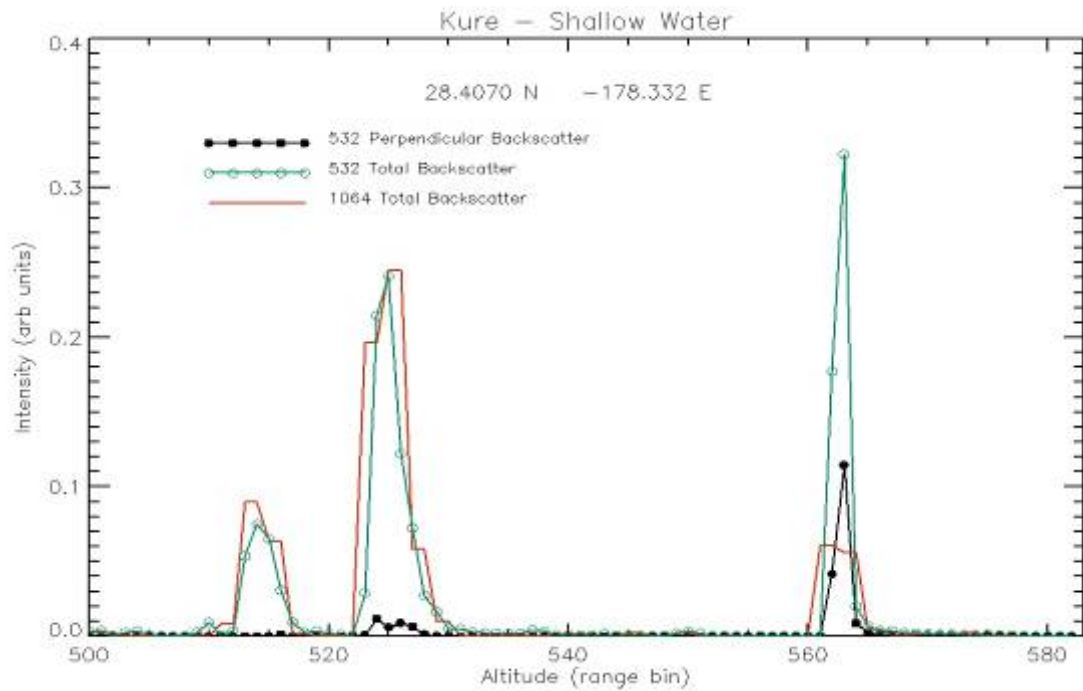


Figure 28. Kure Atoll shallow water

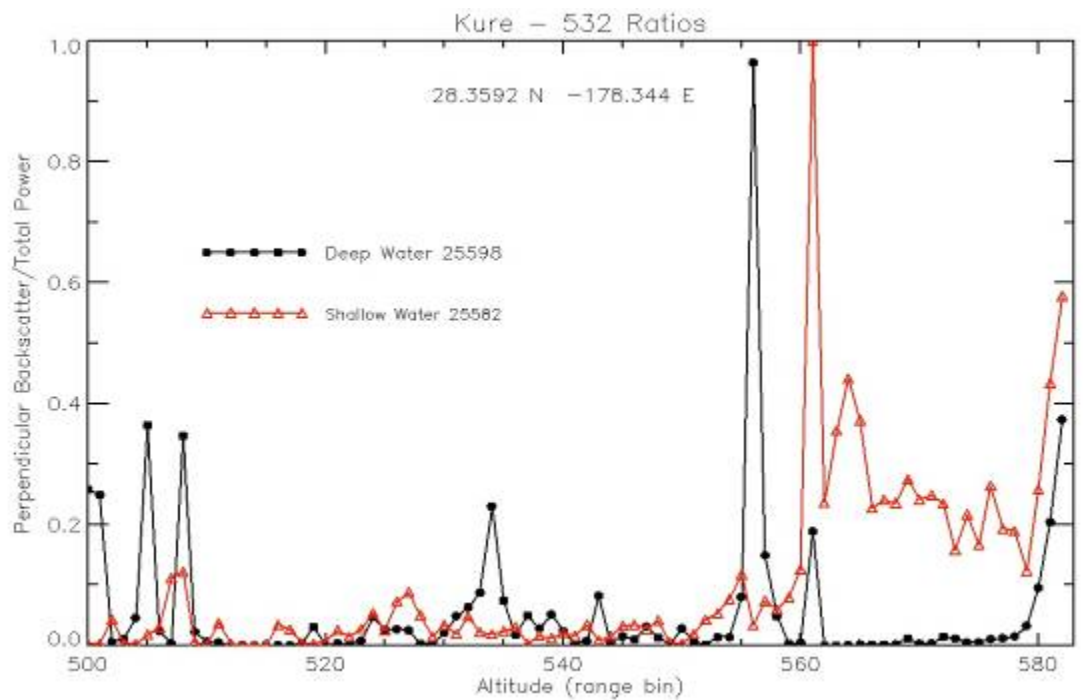


Figure 29. Ratios of Perpendicular 532-nm scatter to total backscatter for shallow water and deep water—Kure Atoll

Since the CALIPSO HDF files had fairly low point density, automation of the analysis using IDL would allow more points to be compared simultaneously thus better revealing any patterns. Figure 30 clearly shows a signature for shallow water that is of a higher intensity than the noise.

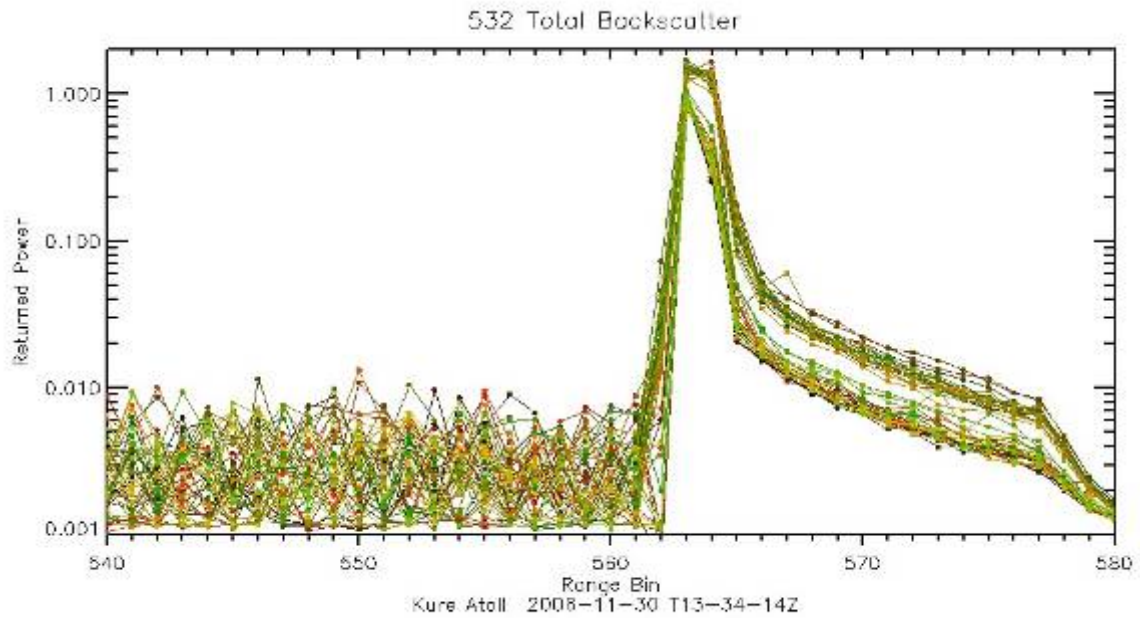


Figure 30. Kure Atoll averaged returned power compared vs. range bin

Figure 31 illustrates the perpendicular backscatter of the 532-nm light. The increase in the perpendicular backscatter seems to indicate shallow water. However, using the ratios of the perpendicular to the total backscatter seemed more likely to give a defining characteristic for shallow water. Figure 32 shows that this ratio is much higher over shallow water.

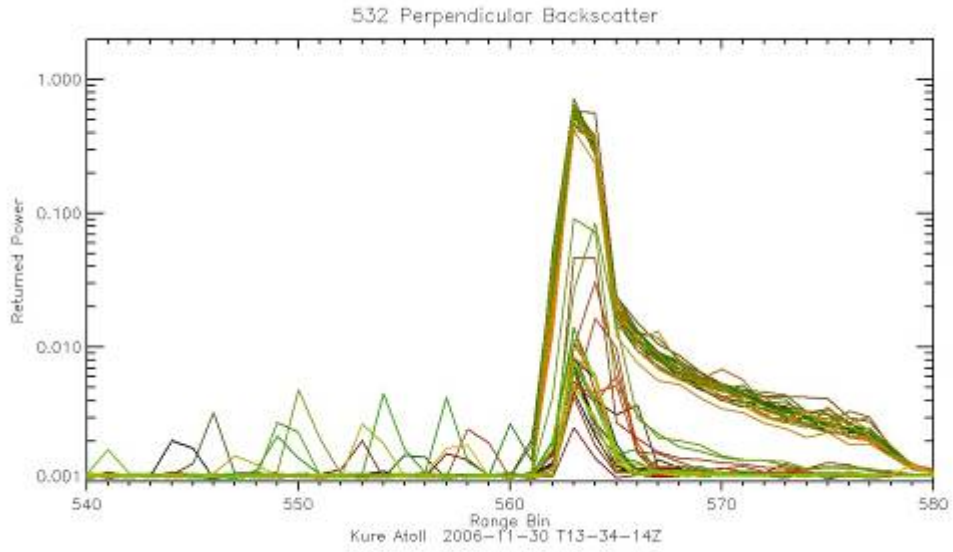


Figure 31. Kure Atoll perpendicular backscatter

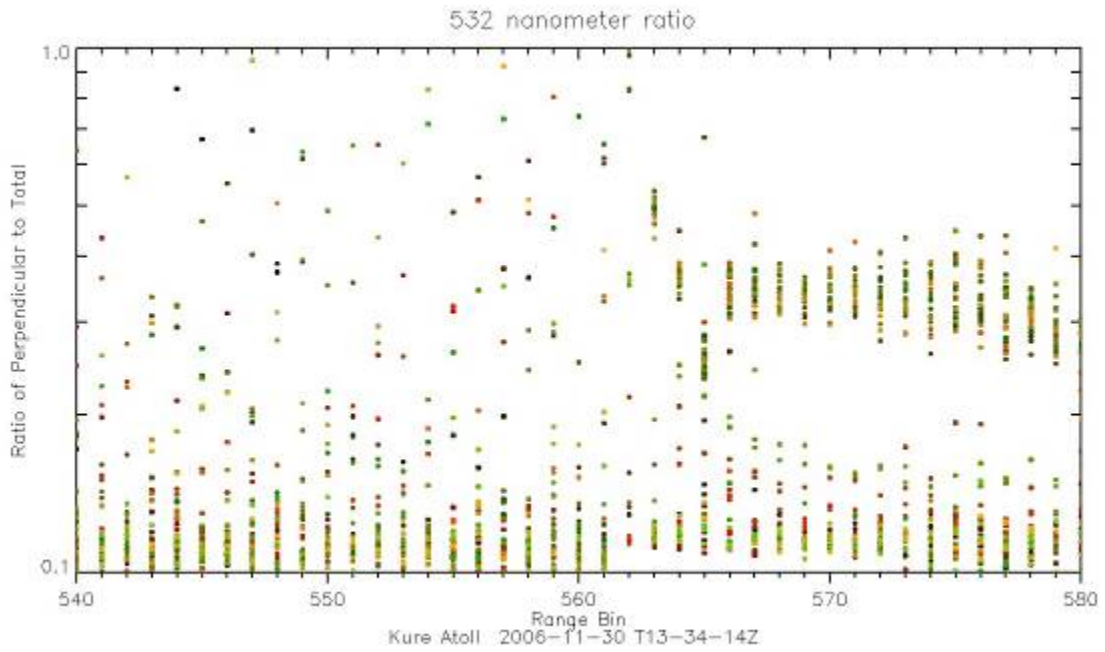


Figure 32. Ratio of perpendicular backscatter to the total backscatter for Kure Atoll

Figure 33 uses averaged data from a Kure Atoll HDF transect and seems to indicate a LIDAR signature that is more clear and less likely to be an instrument artifact. Figure 34 shows that both the perpendicular 532-nm power and the total power both rise over shallow water. Figure 35 then maps out which points over Kure Atoll are classified as shallow or deep.

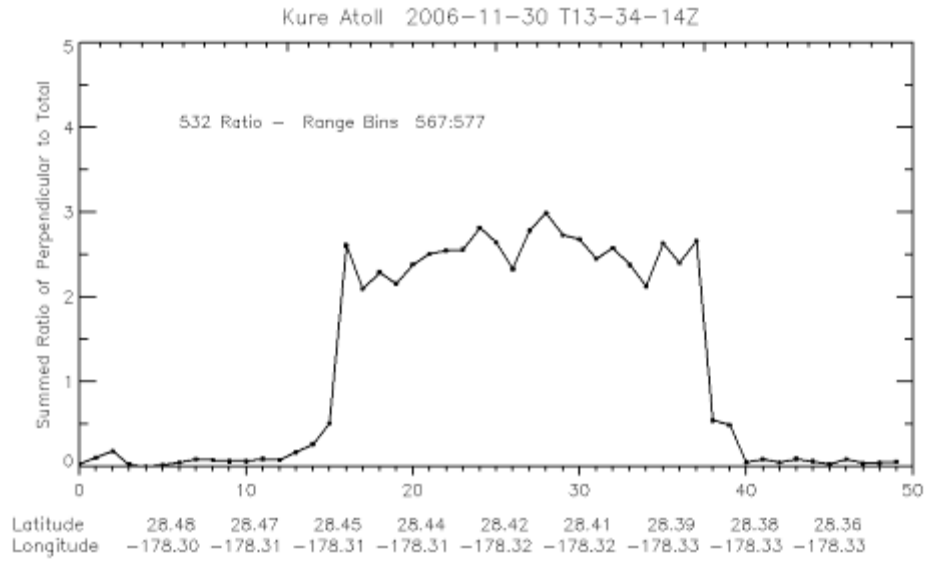


Figure 33. Kure Atoll summed ratio of perpendicular 532-nm light to total

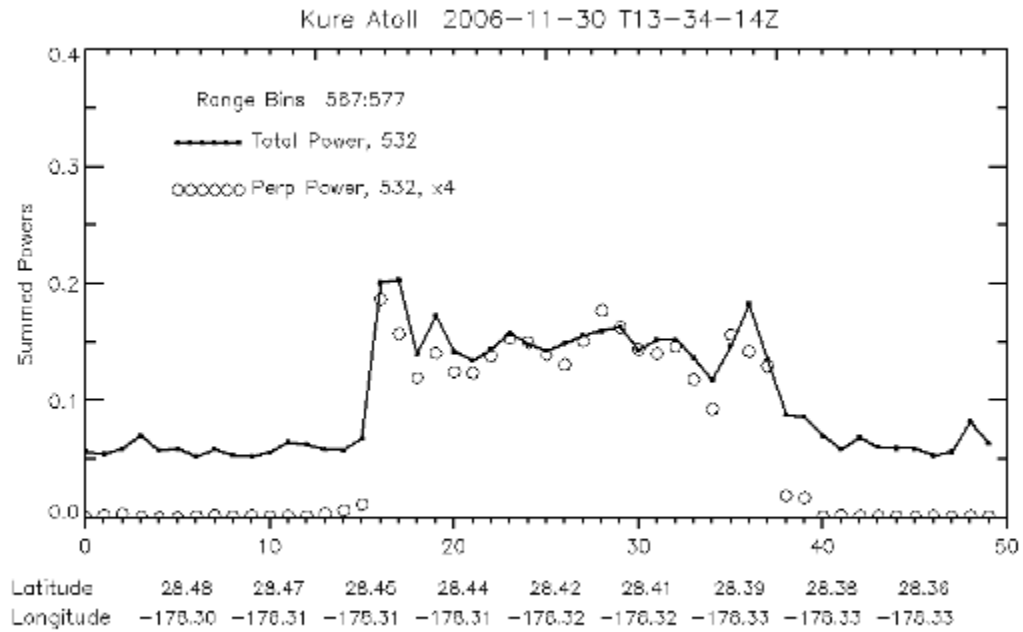


Figure 34. Kure Atoll summed powers of perpendicular 532-nm and total

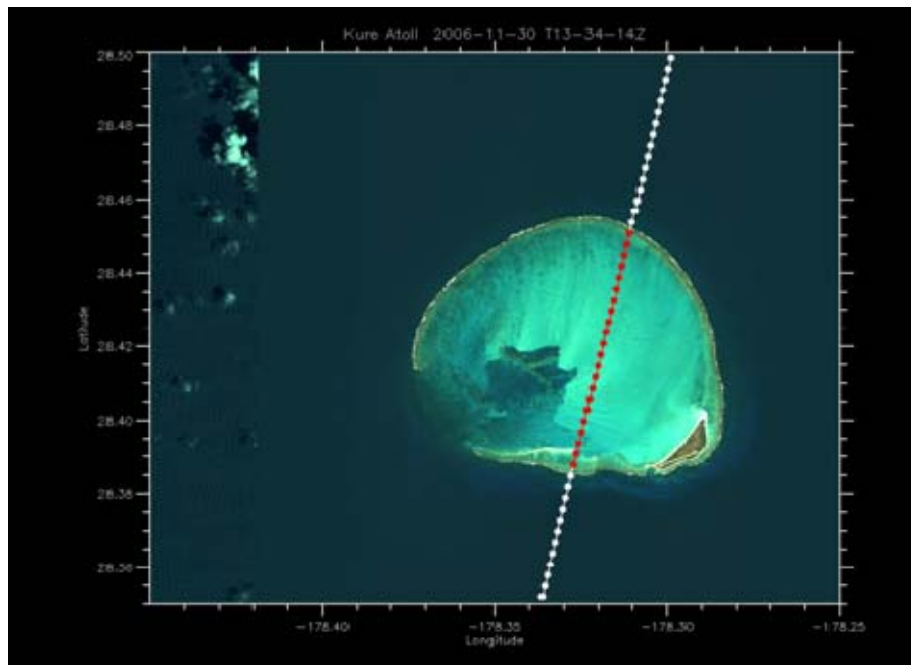


Figure 35. Kure Atoll Quickbird and Landsat background mosaic with depth analysis, red corresponding to shallow water and white with deep water.

After analyzing Kure Atoll, another area was needed to confirm the results. Possibilities included Bora Bora, the Polynesian atolls, Midway, and the Bahamas. A large area with shallow ocean water and possibly more environmental variation would be ideal.

#### **D. THE BAHAMAS**

The Bahamas site was chosen as a second area to analyze – the islands are larger and have variable environments. The CALIPSO transects cross over shallow water, deep water, and land. The Bahamas area was much larger than Kure Atoll and therefore required six Landsat scenes to be connected using the mosaic feature in ENVI. Upon creation of the mosaic, the attributes needed modification to match the data from CALIPSO so Lat/lon projection was selected. Starting with the whole mosaic and then creating subsets with IDL code made this scene more manageable. A peak from the bottom in the 532-nm light return could be seen more clearly in the Bahamas data at certain points. The ratios of reflection data changed a bit more in Bahamas because of increased variation in depth.

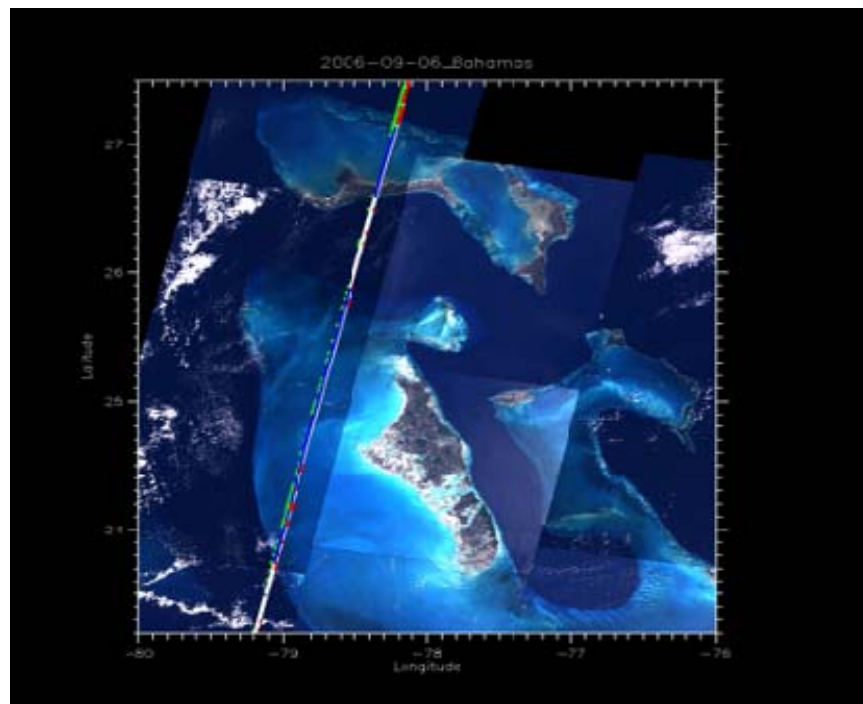


Figure 36. Another Bahamas transect, with color-coded (green/red = clouds, blue = shallow water, white = deep water) regions identified

Analyzing a smaller area made the processing within IDL take less time and, more importantly, avoided crashing the program. The presence of clouds tended to block the light from reaching water, or at least diminishing the effects greatly, so parameters were also set to identify cloud-covered regions.

Beyond identifying cloud cover, thresholds were set for shallow and deep water. After reaching the water, the reflected cross polarized green light (532-nm) is the energy that has penetrated the water. The co-polarized light reflects off the surface of the water and therefore the polarization remains mostly unchanged. It is the cross polarized light that has gone beneath the surface, interacted underwater, and therefore changed polarization.

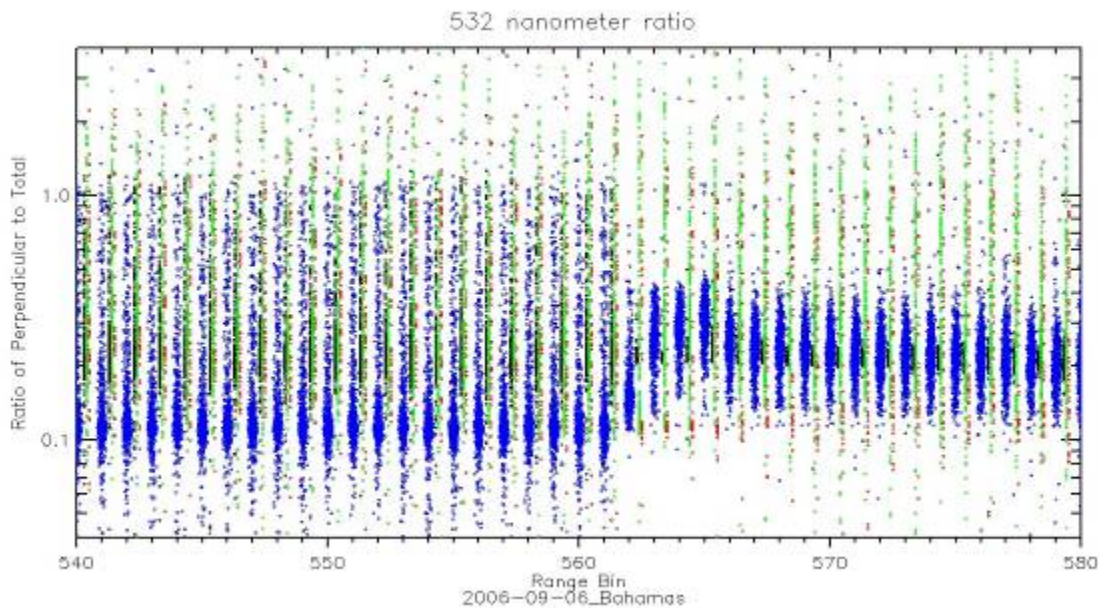


Figure 37. Ratio of perpendicular backscatter to the total backscatter in the Bahamas

To better see the data above the noise, the log scale was used on the vertical axis.

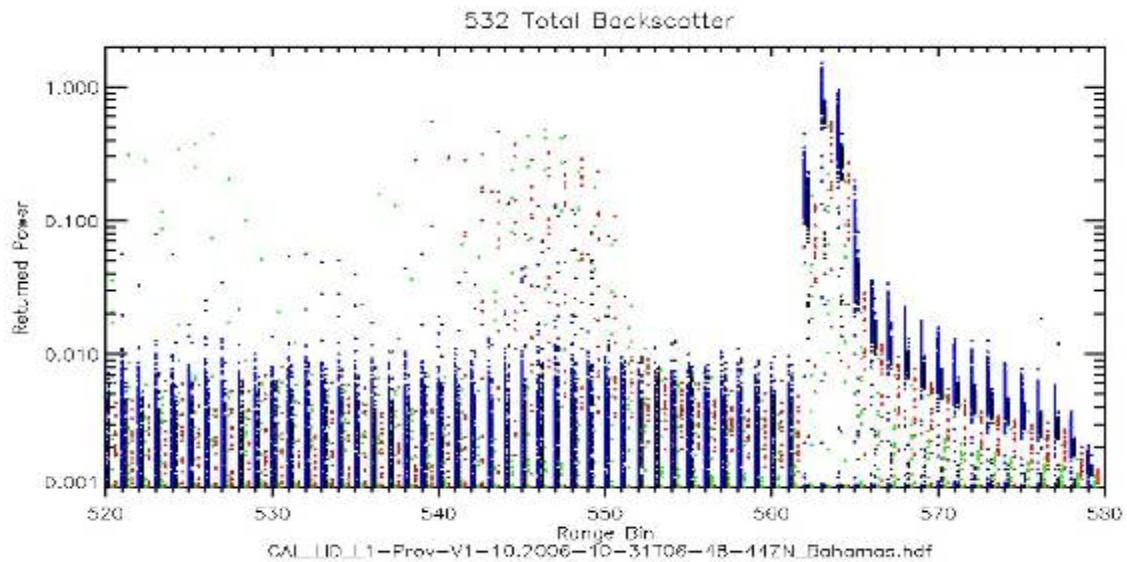


Figure 38. Bahamas “bridge” or “tail” indicating shallow water

After seeing the initial results, it seemed useful to overlay the data from the CALIPSO HDF files on top of visual images to quickly match data with geographic location and visually correlate. For Kure Atoll, data from QuickBird was combined with a Landsat image within ENVI.

A classification scheme of dividing the data by depth and cloud cover was designed. A cloud threshold (greater than .02 sum) identified cloudy areas and a depth threshold identified shallow or deep water. Within IDL, these data types have been designated with a color code:

- Blue—not cloudy, shallow
- Green—cloudy, shallow
- Red—cloudy, deep
- Black/white—not cloudy, deep

## E. SEQUOIAS

A comparison of the Kure Atoll and Bahamas analysis with CALIPSO transects over land areas shows that the water thresholds defined are characteristic to shallow

water. Comparing the ocean areas to both desert and forest clearly showed that the high cross-polarized green light returns corresponded to shallow water. Several transects over the Sequoias contained both desert and forest areas and were thus used as a control measure. The shallow water signature was not present in the Sequoias.

In Figure 39, a characteristic point over the desert in the Sequoias is displayed. There is a sharp spike where the light hits the ground. The return rapidly declines almost immediately after this point.

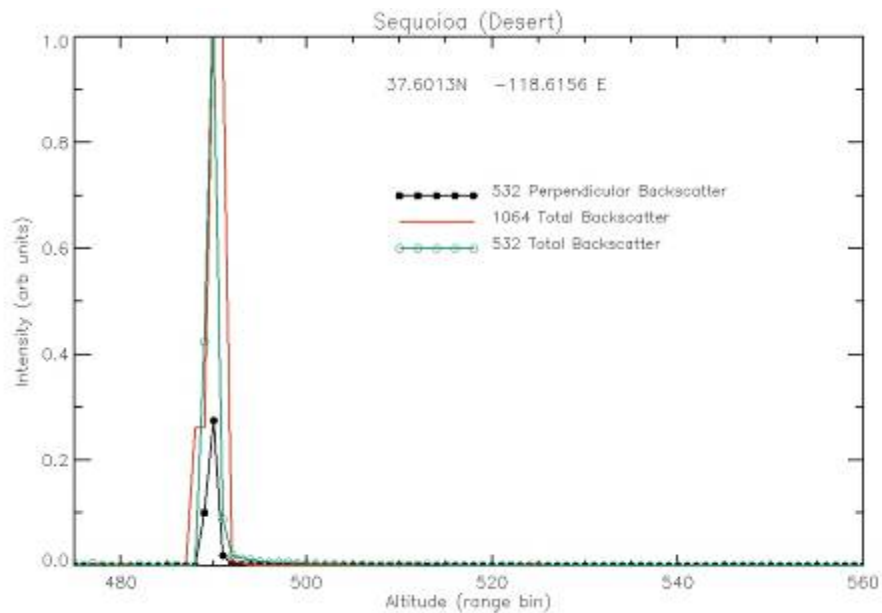


Figure 39. Sequoia backscatter figure over Sequoia desert

In Figure 40, a characteristic point over the forest in the Sequoias is shown. Again, there is a sharp spike where the light hits the forest. Then the light's backscatter drops off, similar to the behavior over the desert.

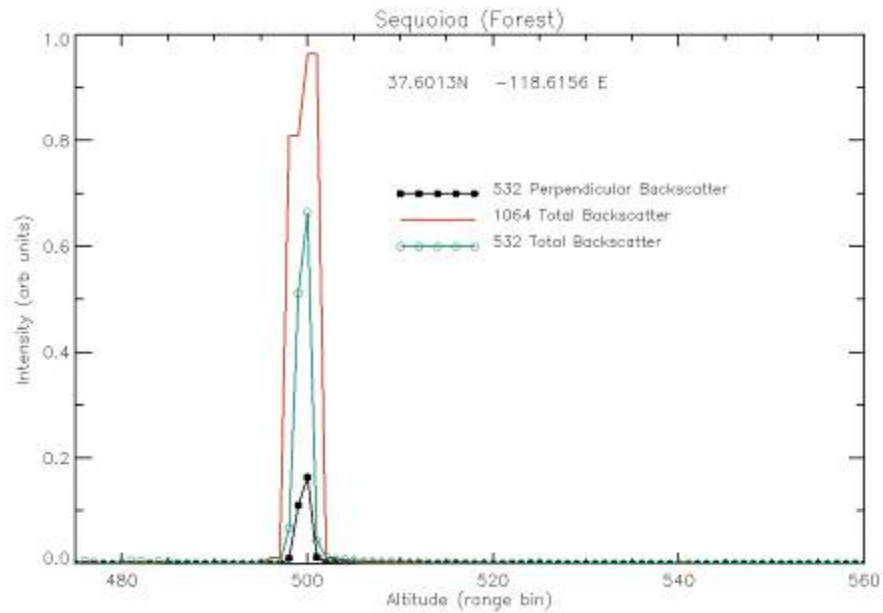


Figure 40. Sequoia backscatter figure over Sequoia forest

Figure 41 shows the ratios of 532-nm cross-polarized light to the total backscatter over both forest and desert in the Sequoias. There is no clear “shallow water” signal for either region in the Sequoias. Figure 42 also shows a lack of the shallow water pattern in the ratios over the Sequoias.

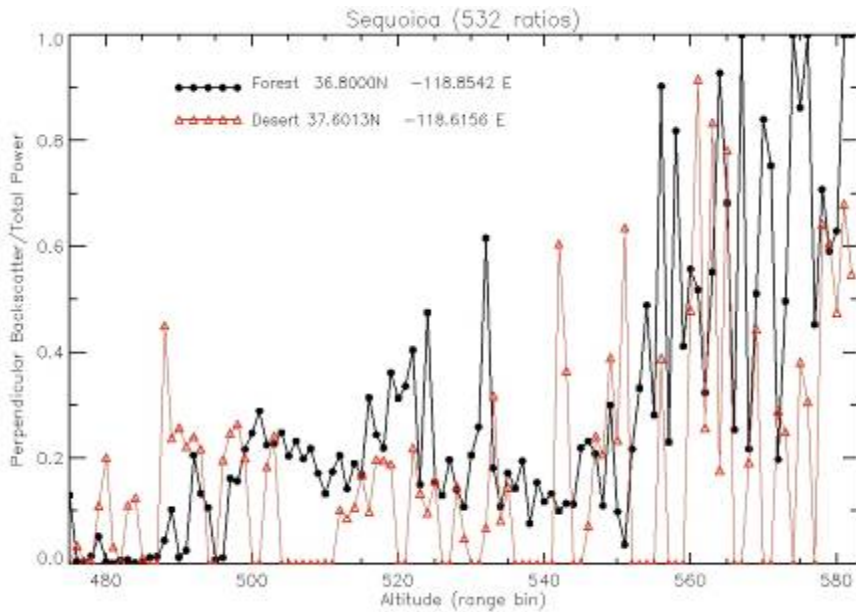


Figure 41. Sequoia backscatter ratios for both desert and forest

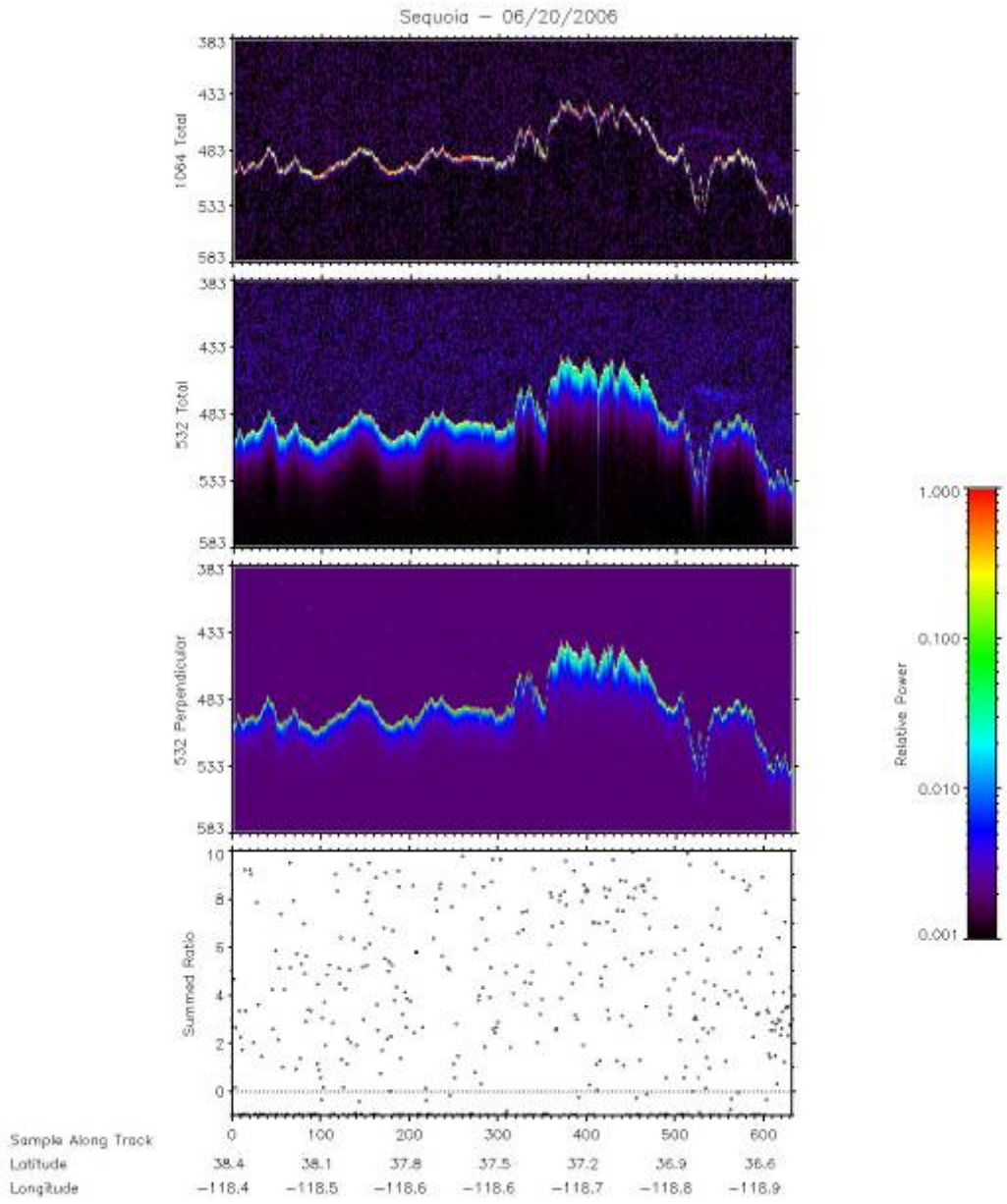


Figure 42. Sequoia spectrogram

## F. COMPARISON TO SPECTRAL BRIGHTNESS

The ENVI software contains a tool that can measure brightness and this attribute correlates qualitatively with water depth. By reading the brightness information from Landsat data, a “pseudo-depth” value can be calculated. The pseudo depths obtained by taking the  $\log_{10}$  of the Landsat Band 1 data. This method follows a variety of similar approaches at NPS and elsewhere (Camacho, 2006). This measurement can then be compared to the CALIPSO backscattered light and polarization information. Ideally, the CALIPSO data would be compared to airborne LIDAR data, as well as ground truth. Since that data has not been used for this research, the pseudo depth has been included for a qualitative comparison of the LIDAR reflectance to depth. In Figure 43, the unclouded region is shown with dense blue points.

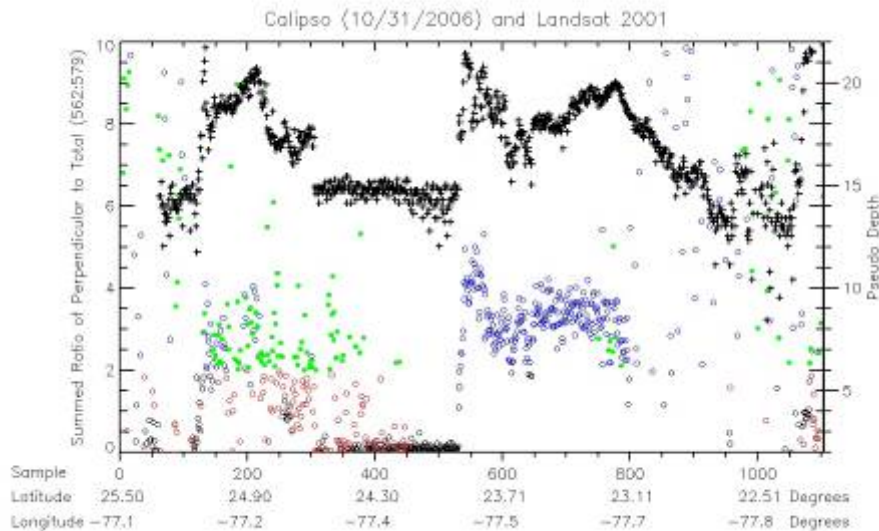


Figure 43. Pseudo depth in black using brightness information from Landsat (over the Bahamas) compared to CALIPSO LIDAR reflectance ratios (in color).

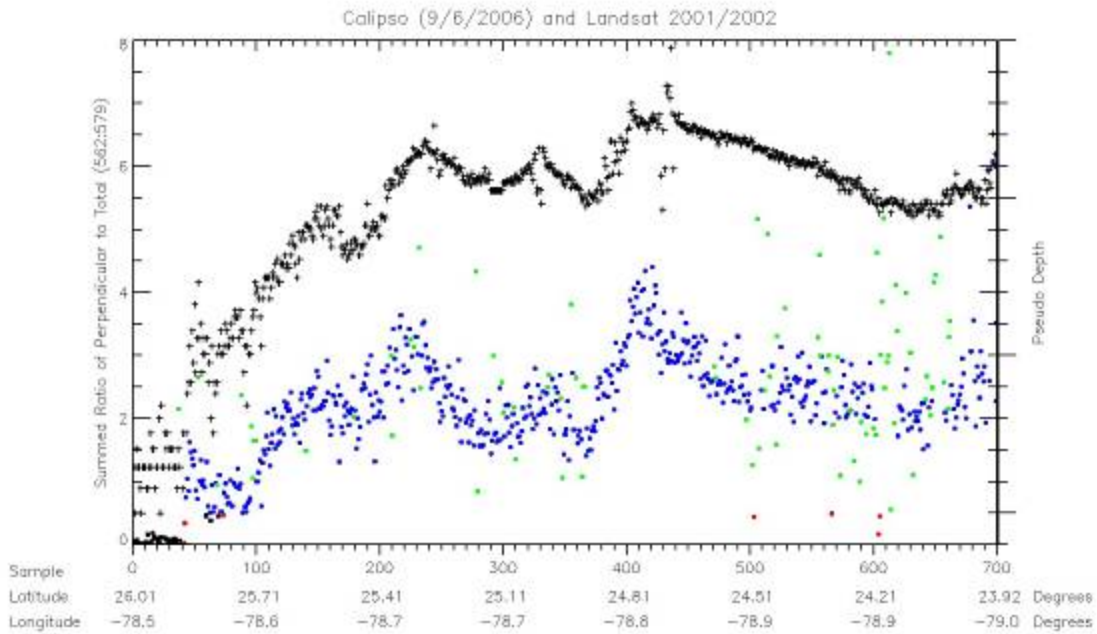


Figure 44. Pseudo depth from Landsat over the Bahamas compared to CALIPSO data from another transect over a more limited area (black from Landsat, and colored points from NASA CALIPSO).

### G. COMPARISON TO BATHYMETRIC NATIONAL OCEAN SURVEY

The CALIPSO data also qualitatively matches to shallow water measurements compiled by the National Ocean Service hydrographic sources. The corresponding area from Figure 36 is placed on Figure 45, and corresponds with the area between the two orange lines. The shallow water above the lines has listed depth measurements of two and four meters, although with coarse contour lines.

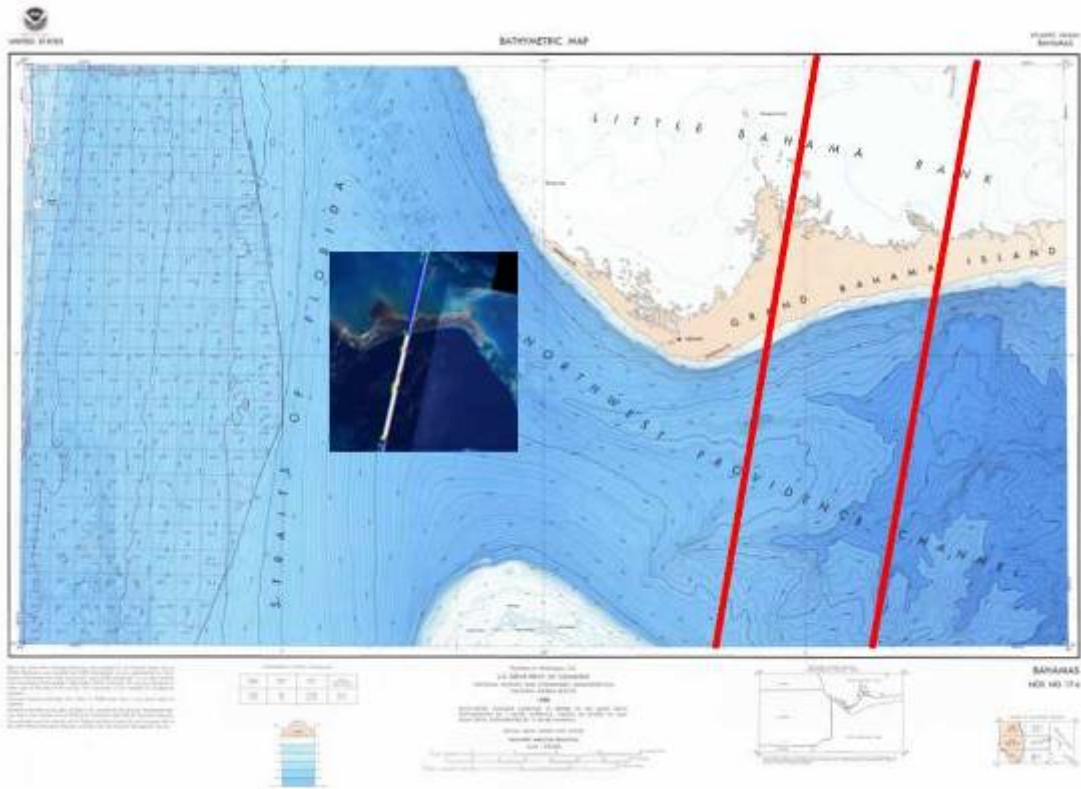


Figure 45. National Ocean Services bathymetric map with section of Figure 36 placed on top (from NOAA NGDC Web site)

THIS PAGE INTENTIONALLY LEFT BLANK

## **V. RESULTS**

### **A. CLASSIFICATION METHODOLOGY AND THRESHOLDS**

The earliest analysis looked at single waveforms that corresponded to individual points along the transect. These waveforms displayed characteristics and patterns that seemed unique to shallow water. However, the CALIPSO waveforms did not have an especially high number of points.

To validate the patterns that seemed present, a number of waveforms were plotted together. The trend of this group more reliably shows the LIDAR signature for shallow water. The ratio of the cross-polarization return from the 532-nm divided by the total backscatter most clearly identifies shallow water.

### **B. CALIPSO'S CAPABILITIES**

CALIPSO can identify shallow water reliably for cloud-free areas at depths of approximately 20 meters. This range is less, but comparable to the distance that airborne LIDAR can see into shallow water. The accuracy of CALIPSO compared to airborne LIDAR systems such as SHOALS, is substantially less.

CALIPSO and other spaceborne LIDAR sensors can serve as useful tools for surveying broad areas of water. Surveying large areas via surface ships and even airborne LIDAR can take prohibitive amounts of time and funding. Spaceborne LIDAR narrow down areas to survey, and help plan airborne LIDAR and surface surveying in a more optimized fashion. The spaceborne LIDAR identifies areas and features that can then be further investigated by airborne and surface sensors.

THIS PAGE INTENTIONALLY LEFT BLANK

## **VI. SUMMARY**

### **A. THESIS RESULTS**

The accuracy of identifying shallow oceanic water with CALIPSO data has been high for cloud-free areas. Spaceborne LIDAR sensing will not replace current airborne or surface sensors, but it can identify some features and help determine where other sensors should survey. LIDAR waveforms offer valuable information because of the different wavelengths being used and polarization features.

### **B. LIDAR SIGNATURE OF SHALLOW WATER**

The ratio of the cross-polarized reflection of green light from the CALIPSO sensor to the total backscatter provides a useful measurement to determine shallow water in the ocean.

### **C. UNANSWERED QUESTIONS**

After completing the research, several unanswered questions remain. The degree to which CALIPSO is close to returning actual depth measurements is unclear. Increases in power could bring spaceborne LIDAR closer to being able to measure depth. The Sequoia Forest was used as a control, but the extent to which CALIPSO can distinguish forest and bare earth, and possibly different types of vegetation, is also unknown.

THIS PAGE INTENTIONALLY LEFT BLANK

## **VII. CONCLUSIONS AND FUTURE WORK**

Using the ratio of the cross-polarized reflection of green light from the CALIPSO sensor to the total backscatter provides a clear indication of the presence of shallow oceanic water. It does not provide accurate bathymetry but, as a wide-area scan, it could be useful to narrow down areas for further surveying. The measurements from CALIPSO can distinguish some features in the ocean, and also serve as a starting point to further investigate others.

THIS PAGE INTENTIONALLY LEFT BLANK

## LIST OF REFERENCES

- Anderson, B.C. (2008). Assessing accuracy in varying LIDAR datapoint densities in digital elevation maps. Master's thesis, Naval Postgraduate School.
- Bretar, F., Chauve, A., Mallet, C., & Jutzi, B. (2008). Managing full waveform LIDAR data: A challenging task for the forthcoming years. Author manuscript, published in "XXI congress, Beijing: China.
- CALIPSO - Cloud-Aerosol LIDAR and Infrared Pathfinder Satellite Observations. (2009). Retrieved 15 December 2009, from NASA Web site: <http://www-calipso.larc.nasa.gov>
- CALIPSO quality statements: Lidar 532-nm detectors transient response (2006). Retrieved 30 March 2010, from NASA Web site: [http://eosweb.larc.nasa.gov/PRODOCS/calipso/Quality\\_Summaries/CALIOP\\_transient\\_response.html](http://eosweb.larc.nasa.gov/PRODOCS/calipso/Quality_Summaries/CALIOP_transient_response.html)
- Camacho, Mark A. (2006). Depth analysis of midway atoll using Quickbird multi-spectral imaging over variable substrates. Master's thesis, Naval Postgraduate School.
- Cassidy, Charles J. (1995). Airborne laser mine detection systems. Master's thesis, Naval Postgraduate School.
- CCMA: Ecosystems: Coral Reefs: Northwest Hawaiian Islands: Kure Atoll: Maps and Imagery. (2009). Retrieved 10 December 2009, from Mobile NOAA site: <http://ccma.nos.noaa.gov/ecosystems/coralreef/nwhi/kure.html>
- Espinoza, F. & Owens, E. R. (2007). Identifying roads and trails hidden under canopy using LIDAR. Master's thesis, Naval Postgraduate School.
- Experimental Advanced Airborne Research Lidar (EAARL). (2009). Retrieved 10 December 2009, from USGS Web site: <http://ngom.usgs.gov/dsp/tech/eaarl/index.html>
- Exton, R. J., Houghton, W. M., Esaias, W., Harriss, R. C., Farmer, F. H., & White, H. H. (1983). "Laboratory analysis of techniques for remote sensing of estuarine parameters using laser excitation," *Appl. Opt.* **22**, 54–64.
- Guenther G. C., Cunningham, A.D., LaRocque, P.E., & Reid, D. J. (2000). Meeting the accuracy challenge in airborne LIDAR bathymetry, *Proc. 20th EARSeL Symposium: Workshop on LIDAR Remote Sensing of Land and Sea*, European Association of Remote Sensing Laboratories, June 16–17, Dresden, Germany, (paper #1 on CD), 28 pp.

- Guenther, G. C. (2007). Digital elevation model technologies and applications : the DEM users manual (2nd ed). Maryland: American Society for Photogrammetry and Remote Sensing.
- Guenther, G. C., Eisler, T. J., Riley, J. L., & Perez, S.W. (1996, June). Obstruction detection and data decimation for airborne laser hydrography, *Proc. 1996 Canadian Hydro. Conf.*, 51–63.
- Hickman, G.D. & Hogg, J. E. (1969). Application of an airborne pulsed laser for near-shore bathymetric measurements, *Remote Sens. of Env.*, 1, 47–58.
- Hochberg, E. J., & Atkinson, M. J. (2000). Spectral discrimination of coral reef benthic communities. *Coral Reefs*, 19, 164–171.
- Hoge, F.E., Wright, C. W., Krabill, W. B., Buntzen, R. R., G.D. Gilbert, G D., Swift, R N., Yungel, J. K., & Berry, R. E. (1988). Airborne LIDAR detection of subsurface oceanic scattering layers, *Appl. Opt.*, 27(19), 3969–3977.
- Irish, J. L. & Lillycrop, W.J. (1999). Scanning Laser Mapping of the Coastal Zone: The SHOALS System, *ISPRS Journal of Photogrammetry & Remote Sensing*, 54(2-3), 123–129.
- J. W. McLean & Freeman, J. D. (1996). “Effects of ocean waves on airborne LIDAR imaging,” *Appl. Opt.* 35, 3261–3269.
- Jensen, Homer (1967). Airborne Photo-Optical Instrumentation, SPIE Proceedings Vol. 8. Edited by Carleton C. Emery. Bellingham, WA: Society for Photo-Optical Instrumentation Engineers, p.8.
- LaRocque P.E., & West, G. R. (1999, October). Airborne laser hydrography: an introduction, *Proc. ROPME/PERSGA/IHB Workshop on Hydrographic Activities in the ROPME Sea area and Red Sea*, 4, 1–15.
- Link, L. E. (1969). Capability of airborne LIDAR profilometer system to measure terrain roughness. In: *Proceedings 6th Symposium Remote Sensing Environment*, Ann Arbor, 15, 189–96.
- Mallet, C. & Bretar, F. (2009). Full-waveform topographic LIDAR: State-of-the-art. *ISPRS Journal of Photogrammetry and Remote Sensing*, 64(1), 1–16.
- McKean, J.; Nagel, D.; Tonina, D.; Bailey, P.; Wright, C.W.; Bohn, C.; & Nayegandhi, A. (2009). Remote Sensing of Channels and Riparian Zones with a Narrow-Beam Aquatic-Terrestrial LIDAR. *Remote Sens. I*, 1065–1096.

- Mobley, C. D., Sundman, L. K., Davis, C. O., Bowles, J. H., Downes, T. V., Leathers, R. A., Montes, M. J., Bissett, W. P., Kohler, D. D. R., Reid, R. P., Louchard, E. M., & Gleason, A. (2005). Interpretation of hyperspectral remote-sensing imagery by spectrum matching and look-up tables. *Applied Optics*, *44*, 3576–3592.
- NASA, CALIPSO. (2010). GLAS ISF Release Notes. Retrieved 10 February 2010, from NASA WFF GLAS Web site: <http://glas.wff.nasa.gov>
- Penny, M.F., Abbot, R. H., Phillips, D. M., Billard, B., Rees, D., Faulkner, D. W., Cartwright, D. G., Woodcock, B., Perry, G. J., Wilsen, P. J., Adams, T. R., & Richards, J. (1986). Airborne laser hydrography in Australia. *Appl. Opt.*, *25*(13): 2046–2058.
- Reitberger, J., Krzystek, P., & Stilla, U. (2006). Analysis of full waveform lidar data for tree species classification. *International Archives of the Photogrammetry, Remote Sensing and Spatial Information Sciences* *36 (Part 3)*, 228–233.
- Shachak Pe'eri, & Philpot, W. (2007). “Increasing the existence of very shallow-water LIDAR measurements using the red-channel waveforms,” *IEEE Trans. Geosci. Remote Sens.*, *45*(5), 1217–1223.
- Vaughan, M. A., Young, S.A., Winker, D. M., Powell, K. A., Omar, A. H., Liu, Z., Hu, Y., & Hostetler, C. A. (2004). Fully automated analysis of space-based LIDAR data: An overview of the CALIPSO retrieval algorithms and data products. *Proc. SPIE Int. Soc. Opt. Eng.*, *5575*, 16–30.
- Wang, C., & Philpot, W. (2007). “Using airborne bathymetric LIDAR to detect bottom type variation in shallow waters,” *Remote Sensing of Environment*, *106*, 123–135.
- Warbington, Ralph; & Beardsley, D. (2002). *2002 Estimates of old growth forests on the 18 national forests of the Pacific Southwest Region*. City of publication: United States Forest Service, Pacific Southwest Region.
- West, G. R., & Lillycrop W. J. (1999). Feature detection and classification with airborne LIDAR—practical experience, *Proc. Shallow Survey-99*, Australian Defence Science and Technology Organization, October 18–20, Sydney, Australia, Paper 3–4, 8 pp.
- WFF GLAS. (2010). Hydropheric and Biospheric Sciences Laboratory News, Retrieved 15 March 2010, from <http://neptune.gsfc.nasa.gov/>
- Winker, D. M., Hunt, W. H., & Hostetler, C. A. (2004). Status and performance of the CALIOP LIDAR. *Proc. SPIE Int. Soc. Opt. Eng.*, *5575*, 8–15.
- Wozencraft, J. M., & Lillycrop, W. J. (2002). *Total shallow-water survey through airborne hydrography*. Paper presented at Oceanology International 2002, Southampton Oceanogr. Cent., London, U. K.

- Y. Hu, Powell, K., Vaughan, M., Tepte, C., Weimer, C., & Behrenfeld, B. (2007). Elevation information in tail (EIT) technique for LIDAR altimetry. *Opt Express* **15** (2007), pp. 14504–14515.
- Y. Hu et al. (2008). Sea surface wind speed estimation from space-based LIDAR measurements. *Atmos. Chem. Phys.*, 8, 3593–2601, 2008.

## INITIAL DISTRIBUTION LIST

1. Defense Technical Information Center  
Ft. Belvoir, Virginia
2. Dudley Knox Library  
Naval Postgraduate School  
Monterey, California
3. Richard C. Olsen  
Naval Postgraduate School  
Monterey, California